Research Article

Journal of Nanoscience, Nanomedicine & Nanobiology

Treatment of Textile Industry Wastewaters with the Addition of Nano-Titanium Dioxide Doped With Nano-Cerium Dioxide

Delia Teresa Sponza[1]* and Rukiye Oztekin[2]

[1]*Environmental Engineering Department, Engineering Faculty, Dokuz Eylül University, Izmir, Turkey*

[2]*Environmental Engineering Department, Engineering Faculty, Dokuz Eylül University, Izmir, Turkey*

Abstract

In this study, the treatment of pollutants (COD_{dis}, color and three polyphenols [4-methyl phenol (C_7H_8O) (4-MP), 4-hydroxyanisole ($C_7H_8O_2$) (4-H), 2-methyl-4-hydroxyanisole ($C_8H_{10}O_2$) (2-M-4-H)] from a textile industry wastewaters with the addition of nano-titanium dioxide doped with nano-cerium dioxide (nano-CeO_2/TiO_2) were intended the different experimental conditions during sonication process. The effects of ambient conditions (25°C), increasing sonication time (120 min and 150 min), increasing sonication temperatures (30°C and 60°C), increasing nano-titanium dioxide (nano-TiO_2) (nano-titania) (0.5, 10 and 20 mg/L), increasing nano-cerium dioxide (nano-CeO_2) (nano-ceria) (10, 100 and 1000 mg/L) and increasing nano-TiO_2 doped with nano-CeO_2 (nano-CeO_2/TiO_2) (100, 500 and 2000 mg/L) (nano-CeO_2/TiO_2 ratios of 1/4, 1/1, 4/1, 9/1, w/w) concentrations on the sonication of wastewater from textile industry wastewater (TI ww) treatment plant in Izmir, Turkey was investigated in a sonicator with a power of 640 W, a frequency of 35 kHz and a sonication time of 150 min for the treatments of Methylene Blue and Rhodamine B dyestuffs. $COD_{dissolved}$, color and three polyphenols [4-methyl phenol (C_7H_8O) (4-MP), 4-hydroxyanisole ($C_7H_8O_2$) (4-H), 2-methyl-4-hydroxyanisole ($C_8H_{10}O_2$) (2-M-4-H)] removal efficiencies were observed during sonication experiments. 99.37% COD_{dis}, 98.07% color, 96% total phenol (PHE R), 93% 4-MP, 88% 4-H and 85% 2-M-4-H maximum removal efficiencies were found in the reactor containing nano-CeO_2/TiO_2=1000 mg/L ([nano-CeO_2=500 mg/L / nano-TiO_2=500 mg/L]=1/1, w/w) after 150 min sonication time at 60°C. The addition of nano-CeO_2/TiO_2 in TI ww was increased to removal efficiencies of pollutions (COD_{dis}, color and polyphenols) higher than the each one of nano-CeO_2 and nano-TiO_2 catalysts additions in TI ww.

Keywords: Nano-cerium dioxide; Nanoparticles; Nano-titanium dioxide; Polyphenols; Sonication; Textile industry wastewater

***Corresponding author:** Delia Teresa Sponza, Faculty of Engıneerıng, Department of Envıronmental Engıneerıng, Department of Envıronmental Scıences, Dokuz Eylül University, Izmir, Turkey, Tel: +90 232 412 11 79, E-mail: delya.sponza@deu.edu.tr

Received Date: May 26, 2021

Accepted Date: May 31, 2021

Published Date: June 12, 2021

Citation: Sponza DT, Oztekin R (2021) Treatment of Textile Industry Wastewaters with the Addition of Nano-Titanium Dioxide doped with Nano-Cerium Dioxide. J Nanosci Nanomed Nanobio 4: 011.

Introduction

The use of nanoparticles (NPs) in water treatment has continuously increased in recent years [1-3]. The production and processing of nanomaterials (NMs) is a quick technology [1]. Metal-oxide nanoparticles (NPs) include nanoscale zinc oxide, titanium oxide, iron oxide, cerium oxide and zirconium oxide, as well as mixed-metal compounds such as indium-tin. In general, NMs are defined as materials of less than 100 nm in size. By the particle size reduction, the surface area of the NPs is increased. Surface activity is a key aspect of NMs. Agglomeration and aggregation blocks surface area from contact with other matter. Only well-dispersed NPs reduces the quantity of NMs [1].

The application of ultrasound (US) as an alternative to the removal of dyes in waters has become of increasing interest in recent years [4,5]. This technique is considered as an Advanced Oxidation Process (AOP) that generates hydroxyl radicals ($OH^{\bullet}$) through acoustic cavitation, which can be defined as the cyclic formation, growth and collapse of microbubbles. Fast collapse of bubbles compresses adiabatically entrapped gas and vapours which leads to short and local hot spots [6]. In the final stage of the collapse, the temperature inside the residual bubble or in the surrounding liquid is thought to be above 5000°C. The $OH^{\bullet}$ and hydroperoxyl radicals ($O_2H^{\bullet}$) can be generated from H_2O and O_2 [7]. Cerium oxide (CeO_2), the most reactive rare earth oxide, is studied and employed in various applications, including catalysts, water splitting in the treatment of pollutions, oxygen storage capacitors and ion conductors [8,9]. CeO_2 are O_2 vacancies and small polarons (electrons localized on cerium cations) because these two are located in the useful range of CeO_2. In the case of O_2 defects, the increased diffusion rate of O_2 in the lattice causes increased catalytic activity as well as an increase in ionic conductivity. As the number of vacancies increases, the ease at which O_2 can move around in the crystal increases, allowing the CeO_2 to reduce and oxidize molecules or co-catalysts on its surface. It has been shown that the catalytic activity of CeO_2 is directly related to the number of O_2 vacancies in the crystal. About 13% phenol and 93% Methylene Blue and 100% Congo Red photodegradation were observed in the case of Fe/Ce ratio of 1/1 ratio [10].

They are many reports of Fe doping on TiO_2 to improve its photocatalytic activity. Amongst a variety of transitional metals, iron has been considered to be an appropriate material due to the fact that the radius of Fe^{+3} (0.79 A) is similar to that of Ti^{+4} (0.75 A), so that Fe^{+3} can be easily incorporated into the crystal lattice of TiO_2. Fe^{+3} has proved to be a successful doping element due to its half-filled electronic configuration [11-15]. Cerium oxides have attracted much attention due to the optical and catalytic properties associated with the redox pair of Ce^{+3}/Ce^{+4}. Ce-doped TiO_2 materials have been synthesized by the sol–gel and hydrothermal methods and used in the pho-

tocatalytic degradation applications. But there are very few reports on Ce doped catalysts and the beneficial effect of Ce doped TiO_2 catalysts are known to depend on different factors, such as the synthesis method and the cerium content [16-18]. The photocatalytic performance of TiO_2 catalysts depends strongly on the methods of metal ion doping and the amount of doping material, since they have a decisive influence on the properties of the catalysts. Therefore, it is necessary to investigate the effects of doping method and doping material content on the photocatalytic performance of TiO_2 nanocatalysts.

There have been many reports of transition metals (Fe, Al, Ni, Cr, Co, W, V and Zr), metal oxides (Fe_2O_3, Cr_2O_3, CoO_2, MgO + CaO and SiO_2), transition metal ceramics (WO_3, MoO_3, Nb_2O_5, SnO_2 and ZnO) and anionic compounds (C, N, and S) being used to dope TiO2 to improve its applicability [11,19-21]. Zeleska [22] has reviewed the preparation methods of doped TiO_2 with metallic and nonmetallic species, including various types of dopants and doping methods. Rauf et al. [23] has given an overview on the photocatalytic degradation of azo dyes in the presence of TiO_2 doped with selective transition metals.

Higher catalytic activity has been reported for the Ce and CeO_2 doped TiO_2 materials for photo-degradation of dyes and other pollutants [16-18]. Titanium dioxide nanopowders doped with visible responsive catalyst may shift the UV absorption threshold of TiO_2 into visible spectrum range and photocatalytic activities can be higher than those of pure TiO_2 and Degussa P25 [12-15,24]. Effect of silver, platinum and gold doping on the TiO_2 for photocatalytic reduction of CO_2 and sonophotocatalytic degradation of methyl orange and organic pollutant nonylphenol ethoxylate has been investigated [25-28]. Also there are reports of tin, calcium, sulfur and zirconia doped TiO_2 being used for photo-degradation of model pollutants [29-32]. Yu et al. [33] synthesized pure TiO_2 particles using ultrasonically-induced hydrolysis reaction and compared the photocatalytic activity of prepared samples with Degussa P 25 and samples prepared by conventional hydrolysis method. Neppolian et al. [34] also prepared nano TiO_2 photocatalysts using sol–gel and ultrasonic-sol–gel methods using two different sources of ultrasonicator, i.e., a bath type and horn type. The effect of ultrasonic irradiation time, power density, the ultrasonic sources (bath-type and horn-type), magnetic stirring, initial temperatures and sizes of the reactors has been investigated. Li et al. [35] used the combination of ultrasonic and hydrothermal method for preparing Fedoped TiO_2 for photo-degradation of methyl orange. Zhou et al. [12] used ultrasonicaly-induced hydrolysis reaction for the preparation of Fe-doped TiO_2 whereas Huang et al. [36] synthesized and characterized Fe_xO_y-TiO_2 via the sonochemical method.

The synthesis of metal-loaded semiconductor oxide materials by conventional physical blending or chemical precipitation followed by surface adsorption usually yields insoluble materials for which the control over size, morphology and dispersion of the metal component remains inherently difficult. These methods often require a long time and are inherently multi-step procedures. Sonochemistry has been proven to be an excellent method for the preparation of mesoporous materials. The physical and chemical effects generated by acoustic cavitation can be expected to significantly influence the properties of doped materials [12,26]. Ultrasound has been very useful in the synthesis of a wide range of nanostructured materials, including high-surface area transition metals, alloys, carbides, oxides, and colloids. The collapse of cavitation bubbles generates localized hot spots with transient temperature of about 10000°K (9726.850°C), pressures of about 1000 atm or more and cooling rates in excess of 109 K/s. Under such extreme conditions, various chemical reactions and physical changes occur and numerous nano-structured materials such as metals, alloys, oxides and biomaterials can be effectively synthesized with required particle size distribution [12,37-39]. In the past the sonochemical method has been applied to prepare various TiO_2 and doped nanomaterials and photocatalytic activity has been evaluated by different researchers [33-36,40,41].

The results of the photocatalytic degradation of various pollutants which can be present in industrial wastewater prove the purposefulness of CeO_2 doping with metal and non-metal dopants [42]. The doping resulted in the following: (1) The formation of surface defects, which prevented electron-hole recombination or decreased recombination rates; (2) an increase in the surface area and a higher number of sites accessible for the adsorption of pollutants on CeO_2 particles; (3) a decrease in the band gap energy, leading to visible light absorption; and (4) higher photocatalytic activity of pollutant degradation [42]. All results also showed that coupling TiO_2 with CeO_2 could produce special electrons and holes transfer from TiO_2 to CeO_2 which is able to facilitate the separation of the electron–hole pairs and therefore, improve photocatalytic activity of the hybrid photocatalyst [42].

Liu and Sun [43] investigated the degradation of an azo dye, Methyl Orange, in catalytic wet air oxidation process with Fe_2O_3-CeO_2-TiO_2/γ-Al_2O_3 as catalyst at a room temperature in a synthetic wastewater containing 500 mg/L Methyl Orange. 98.09% of color and 96.08% of TOC was removed in 150 min [43]. Also, the influences of heat-treatment temperature (300, 500 and 700°C) and heat-treatment time (20, 60, and 100 min) on the sonocatalytic activities of CeO_2/TiO_2, SnO_2/TiO_2 and ZrO_2/TiO_2 composites, and of irradiation time (20, 40, 60, 80 and 100 min) and solution acidity (pH=3-5-7-9-11) on the sonocatalytic degradation of Acid Red B was investigated. The Acid Red B decreases was in order: in CeO2/TiO_2>67.41%, in SnO_2/TiO_2>65.26%, in TiO_2>41.67%, in ZrO_2/TiO_2>28.34%, in SnO_2>26.75%, in CeO_2>23.33%, in ZrO_2>16.67% with only US respectively, at pH=5 after 60 min sonication time. Methyl Violet color removals were observed as 40% in TiO_2, 25% in ZrO_2/TiO_2, 55% in SnO_2/TiO_2, 50% in CeO_2/TiO_2, respectively. Chen and Liu [20] investigated the effects of CeO_2-ZnO composite nanofibers on the treatment of organic-polluted H_2O, Photocatalytic activity experiments showed that the Rhodamine B was almost completely decomposed when it was catalyzed by CeO_2-ZnO NFs within 180 min, while only 17.4% and 82.3% of this dye was decomposed under catalysis by sole CeO_2 and sole ZnO NFs, respectively [20].

TiO_2 is broadly used in environmental clean-up operations because of its non-toxic nature, photochemical stability and low cost [44,45]. TiO_2 has a large band gap energy, more than 3.0 eV, and relatively long electron-hole pair recombination time [46-48]. To achieve rapid and efficient decomposition of organic pollutants and also easy manipulation of the catalyst in a total sonication process, it may be effective to load TiO_2 NPs onto suitably fine adsorbents and thus concentrate pollutants around the NPs. Doping metal elements into TiO_2 may also strain the recombination of electron-hole pairs. The strong oxidative potential of the positive holes oxidizes H_2O to create $OH^{\bullet}$ radicals. In a study performed by Entezari and Petrier [49] 50-60% phenol removals was obtained after 45 min sonication time, at 423 kHz, at TiO_2=8 mg/L and at 60°C. They reported that the $OH^{\bullet}$ produced by US can react with phenol resulting in a dephenolization process [49]. In a study performed by Khochwala and Gogate [50] it has

been observed that 2000 mg/L TiO_2 is the optimum concentration for 78% phenol removal in olive mill industry wastewater (OMW). Wu et al. [51,52] have reported similar results for degradation of phenol and trichloroacetic acid in a combined operation involving two 9 W H-shaped ultraviolet (UV) lamps and an ultrasonic horn operating at 30 kHz and at 100 W in OMW. Kidak and Ince [53] and Shirgaonkar and Pandit [54] have also reported 78% and 79% degradation yields for phenol and 2, 4, 6-trichlorophenol, respectively, in the presence of 450 mg/L TiO_2 in the OMW. An anatase TiO_2 was used to remove the Aromatic Amines (AAs) namely, 4, 4-oxydianiline with a yield 85% from OMW after 120 min sonication time. 87% mineralization of AAs was achieved in a study performed by Cardoso et al. [55]. In a study performed by Mrowetz et al. [56] 36% COD removal was found in a TI ww containing 75 mg/L Acid Orange 8, at 20 kHz, at 250 W, in TiO_2=100 mg/L, after 100 min sonication time and at 35°C. Wang et al. [57] obtained 60% color yield in a TI ww containing 100 mg/L Azo Funchsine solution at 40 kHz, at 50 W, after 60 min sonication time, at 30°C with TiO_2=50 mg/L. In a study performed by Abbasi and Asl [58] 90% colour removal was achieved in a TI ww containing 15 mg/L Basic Blue 41, at 35 kHz, at 160 W, after 180 min sonication time, at 30°C with TiO_2=100 mg/L. In a study performed by Wu and Yu [59] 63% Total Aromatic Amines (TAAs) removal was accomplished in a TI ww containing 20 mg/L C.I. Reactive Red 2 in TiO_2=2000 mg/L, at 40 kHz, at 400 W, at 10 W/cm^2, after 120 min sonication time, at pH=7.0 and at 60°C.

The studies performed until now with real TI ww were not concern the removals of color originated from Methylene Blue and Rhodamine B and of polyphenols with nano-titanium dioxide doped with nano-cerium dioxide throughout sonication. The novelty of this study is the removals of s 4-methyl phenol, 4-hydorxyanisole and 2-methyl-4-hyroxyanisole, color and tdissolved COD with nano-CeO_2 doped TiO_2. Therefore, in the peresent study, the effects of ambient conditions (25°C), increasing sonication time (120 and 150 min), sonication temperature (30°C and 60°C), nano-titanium dioxide (nano-TiO_2) (nano-titania) (0.5, 10 and 20 mg/L), nano-cerium dioxide (nano-CeO_2) (nano-ceria) (10, 100 and 1000 mg/L) and nano-TiO_2 doped with nano-CeO_2 at nano-CeO_2/TiO2 ratios of 1/4, 1/1, 4/1 and 9/1 on the sonication of the wastewater from TI ww treatment plant in Izmir, Turkey was investigated in a sonicator with a power of 640 W, a frequency of 35 kHz and a sonication time of 150 min. COD_{dis}, color and three polyphenols [4-methyl phenol (C_7H_8O) (4-MP), 4-hydroxyanisole ($C_7H_8O_2$) (4-H), 2-methyl-4-hydroxyanisole ($C_8H_{10}O_2$) (2-M-4-H)] removal efficiencies were observed during sonication experiments.

Material and Methods

Raw wastewater

The TI ww used in this study contains color (>70.9 1/m), total phenol (>37 mg/L), COD_{dis} (>770 mg/L) and high BOD_5 (>251 mg/L) concentrations with a BOD_5/COD_{dis} ratio of 0.33. The characterization of TI ww was shown in Table 1 for minimum, medium and maximum values.

Configuration of sonicator

A BANDELIN Electronic RK510 H sonicator was used for sonication of the TI ww samples. The sonication frequency and the sonication power were 35 kHz and 640 W, respectively. Glass serum bottles in a glass reactor were filled to a volume of 100 mL with raw TI ww and they were closed with teflon coated closers for the measurement of volatile compounds (evaporation) of the raw TI ww. The evaporation losses of volatile compounds were estimated to be 0.01% in the reactor and, therefore, assumed to be negligible. The serum bottles were filled with 0.1 mL methanol in order to prevent adsorption on the walls of the bottles and minimize evaporation. 25°C, 30°C and 60°C temperatures were adjusted electronically in the sonicator with two thermostatic heaters. The stainless steel sonicator was equipped with a teflon holder to prevent temperature losses. The shematic configuration of the sonicator used in this study is shown in Figure 1.

Parameters	Values		
	Minimum	Medium	Maximum
pH	5 ± 0.18	5.27 ± 0.19	6 ± 0.21
DO (mg/L)	1.30 ± 0.05	1.40 ± 0.05	1.50 ± 0.05
ORP (mV)	85 ± 2.98	106 ± 3.71	128 ± 4.48
TSS (mg/L)	285 ± 9.98	356 ± 12.46	430 ± 15.05
TVSS (mg/L)	192 ± 6.72	240 ± 8.40	290 ± 10.15
CODtotal (mg/L)	931.70 ± 32.61	1164.60 ± 40.76	1409.20 ± 49.32
CODdissolved (mg/L)	770.40 ± 26.96	962.99 ± 33.71	1165.22 ± 40.78
TOC (mg/L)	462.40 ± 16.18	578 ± 20.23	700 ± 24.50
BOD5 (mg/L)	251.50 ± 8.80	314.36 ± 11	380.38 ± 13.31
BOD5/CODdis	0.26 ± 0.01	0.33 ± 0.012	0.40 ± 0.014
Total N (mg/L)	24.80 ± 0.87	31 ± 1.09	37.51 ± 1.31
NH4-N (mg/L)	1.76 ± 0.06	2.20 ± 0.08	2.66 ± 0.09
NO3-N (mg/L)	8 ± 0.28	10 ± 0.35	12.10 ± 0.42
NO2-N (mg/L)	0.13 ± 0.05	0.16 ± 0.06	0.19 ± 0.07
Total P (mg/L)	8.80 ± 0.31	11 ± 0.39	13.30 ± 0.47
PO4-P (mg/L)	6.40 ± 0.22	8 ± 0.28	9.68 ± 0.34
Total phenol (mg/L)	29.60 ± 1.04	37 ± 1.30	44.80 ± 1.57
SO4-2 (mg/L)	1248 ± 43.70	1560 ± 54.60	1888 ± 66.10
Color (1/m)	70.90 ± 2.48	88.56 ± 3.10	107.20 ± 3.75
TAAs (mg benzidine/L)	1296 ± 45.36	1620 ± 56.70	1960 ± 68.60

Table 1: Characterization values of TI ww (n=3, mean values ± SD).

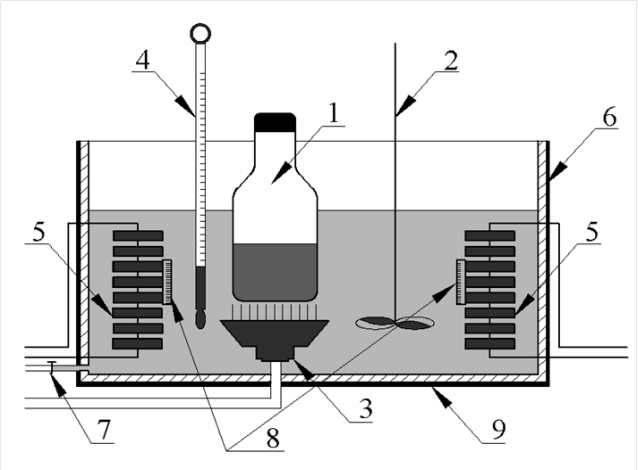

Figure 1: The structural diagram of the sonicator used in this study: (1) glass reactor, (2) stirrer, (3) energy conversion device, (4) thermometer, (5) heater, (6) stainless steel bath, (7) water exit valve, (8) thermostate, (9) teflon cover.

Operational Conditions

The effects of ambient conditions (25°C), increasing sonication time (120 and 150 min), sonication temperature (30°C and 60°C), nano-titanium dioxide (nano-TiO_2) (nano-titania) (0.5, 10 and 20 mg/L), nano-cerium dioxide (nano-CeO_2) (nano-ceria) (10, 100 and 1000 mg/L) and nano-TiO_2 doped with nano-CeO_2 (nano-CeO_2/TiO_2) (100, 500 and 2000 mg/L) concentrations on the sonication of wastewater from textile industry wastewater (TI ww) treatment plant in Izmir, Turkey was investigated. Fresh solutions of nano-TiO_2 (>99% purity, Merck, Germany) and nano-CeO_2 (>99% purity, Merck, Germany) were added to the TI ww by an peristaltic pump (Watson-Marlow Bredel pumps, USA) with a flow rate of 0.1 mL/min through 5 min before US was begun at pH=5.4. Sonicated samples were taken at 120th and 150th min of sonication time and were kept in a refrigerator with a temperature of +4°C for experimental analysis. Deionized pure H_2O (R ¼ 18 MΩ/cm) was obtained through a SESA Ultrapure water system.

All experiments were in batch mode by using an ultrasonic transducer (horn-type), which has five adjustable active acoustical vibration areas of 12.43, 13.84, 17.34, 26.4 and 40.69 cm^2, with diameters 3.98, 4.41, 4.7, 5.8 and 7.2 cm, with input US powers of 120, 350, 640, 3000 and 5000 W, with US frequencies of 25, 35, 132, 170 and 350 kHz, with US intensities of 15.7, 24.2, 36.9, 46.2 and 51.4 W/cm^2, with power densities of 0.1, 0.9, 1.65, 1.9, 2.14 W/mL, with specific energies of 2.4, 3.1, 4.1, 5.1, 11.5 kWh/kg. $COD_{influent}$, respectively, were chosen to identify for maximum removal of pollutant parameters (COD_{dis}, color, total phenol and polyphenols) in the TI ww at the bottom of the reactor through a piezoelectric disc (4-cm diameter) fixed on a pyrex plate (5-cm diameter) (see Table 2). Samples were taken after 120th and 150th min of US time and they were analyzed immediately.

Ultrasound parameters	Values				
Ultrasound frequency (kHz)	25	35	132	170	350
Ultrasound power (W)	120	640	350	3000	5000
Power density (W/mL)	0.1	2.14	0.9	1.65	1.9
Ultrasound intensity (W/cm2)	15.7	51.4	24.2	36.9	46.2
Specific energy (kWh/kg CODinfluent)	2.4	11.5	3.1	4.1	5.1
Active acoustical vibration area (cm2)	12.43	40.69	13.84	17.34	26.4
Reactor diameters (cm)	3.98	7.2	4.41	4.7	5.8
COD removal efficiency (%)	45	61	47	53	58

Table 2: Sonicational parameters and corresponding values of sonication process in this study at pH=5.4 after 150 min sonication time for maximum COD_{dis} yields under ambient conditions (at 25oC), at initial COD_{dis} concentrations=962,99 mg/L, at sonication power=640 W and at sonication frequency=35 kHz (n=3, mean values).

Reagent grade perfluorohexane (C_6F_{14}) was taken from Fluka (Germany). Aniline (99%), 2-PHE (99%), 3-PHE (99%), 2, 4, 6 trimetylaniline (99%), dimethylaniline (99%) and o-toluidine (99%) was purchased from Aldrich (USA).

Analytical Methods

pH, T(°C), ORP (mV), TSS, TVSS, DO, BOD5, COD_{total}, $COD_{dissolved}$, TOC, oil were monitored following Standard Methods 2550, 2580, 2540 C, 2540 E, 5210 B, 5220 D, 5310, 5520 B, respectively [60]. Total-N, NH4-N, NO_3-N, NO_2-N, Total-P, PO_4-P, total phenol and SO_4-2 were measured with cell test spectroquant kits (Merck, Germany) at a spectroquant NOVA 60 (Merck, Germany) spectrophotometer (2003). The characterization of TI ww was shown in Table 1 for minimum, medium and maximum values.

Chemical Oxygen Demand (COD) Measurements

COD was determined with Close Reflux Method following the Standard Methods 5220 D [60] using an Aquamate thermo electron corporation UV visible spectrophotometer (2007). First the samples were centrifuged for 10 min at 7000 rpm. Secondly, 2.50 mL volume samples were treated with 1.50 mL 10216 mg/L $K_2Cr_2O_7$ with 33.30 g/L $HgSO_4$ and 3.50 mL 18.00 M H_2SO_4 which contains 0.55% (w/w) Ag_2SO_4. Thirdly the closed sample tubes were stored in a 148°C heater (thermoreactor, CR 4200 WTW, 2008) for 2 hour (h). Finally, after cooling, the samples were measured at 600 nm with an Aquamate thermo electron corporation UV visible spectrophotometer (2007). The Close Reflux Method COD was used to measure the COD in TI ww before and after sonication experiments.

Total COD (CODt)

Wastewater samples were used to measure the total COD (COD_t) in TI ww before and after sonication process.

Dissolved COD (COD_{dis})

0.45 µm membrane-filtered (Schleicher & Schuell ME 25, Germany) wastewater samples were used to measure the dissolved COD (COD_{dis}) in TI ww prior and after sonication experiments.

Total Organic Carbon (TOC) Measurements

TOC was measured following the Standard Methods 5310 [60] with a Rosemount Dohrmann DC-190 high-temperature total organic carbon (TOC) analyzer (1994).

Colour Measurements

In the studies with real colorful TI ww which is including Methylene Blue ($C_{16}H_{18}N_3SCl$). The measurement of color was carried out following the approaches described by Olthof and Eckenfelder [61] and Eckenfelder [62]. According these methods, the color content was determined by measuring the absorbance at three wavelengths (445 nm, 540 nm and 660 nm), and taking the sum of the absorbances at these wavelengths. To convert the absorbance into (1/m) the equation given below Equation (1) was used.

$$\alpha = \left(\frac{A}{d}\right) f \qquad (1)$$

Where;

A: Color in (1/m) unit,

A: Measured absorbance value from the spectrophotometer,

D: Sample length (cell width, 10 mm),

F: Factor (1000).

Raw wastewater was diluted with deionized H_2O between 100 and 1000 mg/L at ten different concentrations for the calibration graphic and calibration equation of color measurement. These ten different wastewater concentrations were measured at three different wavelents

(445 nm, 540 nm and 660 nm) with an Aquamate thermo electron corporation UV visible spectrophotometer (2007). Results of three different wavelents were illustrated in Table 3, Table 4 and Table 5. Three different calibration in Equations (2), (3) and (4) were obtained for color measurement at three different wavelents (445 nm, 540 nm and 660 nm).

Concentrations (mg/L)	Absorbance (nm)
100	0.098
200	0.199
300	0.296
400	0.412
500	0.534
600	0.591
700	0.705
800	0.816
900	0.910
1000	0.998

Table 3: Standard concentrations (mg/L) versus absorbance (nm) values of color A1:445 nm (λ = 445 nm) using an Aquamate thermo electron corporation UV visible spectrophotometer (2007).

Concentrations (mg/L)	Absorbance (nm)
100	0.102
200	0.214
300	0.313
400	0.428
500	0.507
600	0.653
700	0.711
800	0.826
900	0.900
1000	0.994

Table 4: Standard concentrations (mg/L) versus absorbance (nm) values of color A2:540 nm (λ = 540 nm) using an Aquamate thermo electron corporation UV visible spectrophotometer (2007).

Concentrations (mg/L)	Absorbance (nm)
100	0.091
200	0.197
300	0.302
400	0.401
500	0.523
600	0.630
700	0.724
800	0.812
900	0.927
1000	0.990

Table 5: Standard concentrations (mg/L) versus absorbance (nm) values of color A3:660 nm (λ = 660 nm) using an Aquamate thermo electron corporation UV visible spectrophotometer (2007).

$$y = 1.0068 * X + 2.133 \qquad R^2 = 0.9983 \qquad (2)$$

$$y = 0.9933 * X + 8.467 \qquad R^2 = 0.9968 \qquad (3)$$

$$y = 1.0198 * X - 1.2 \qquad R^2 = 0.9979 \qquad (4)$$

Polyphenol Measurements

Polyphenol measurement was performed following the Standard Methods 5520 B [60]. Firstly, 5 ml of TI ww sample was added in 40 mL dark brown color Amber I-cem vial (Catalog number: 98716). Secondly, 5 mL of mixture of siklohexane (50%) and etilacetate (50%) was added on 5 mL of TI ww sample in 40 mL dark brown color Amber I–cem vial. After, this solutions were mixtured at 15 min. Upper part of mixtured solution was taken with a pasteur pipette in a new 40 mL dark brown color Amber I–cem vial. 0.50 g Na_2SO_4 chemical was added for waterless condition in a new 40 mL dark brown color Amber I–cem vial. After that, this 40 mL dark brown color Amber I–cem vial again was mixtured at 15 min. The upper part of 40 mL dark brown color Amber I–cem vial was taken with a Pasteur pipette in a 1.5 mL of colorless glass vial (Agilent). 1 mL sample was added in a 1.5 mL of colorless glass vial for GC-MS analysis. Polyphenol was analysed with a gas chromotography (Agilent 6890) combined with a mass selective detector (Agilent 5973 inert MSD). A capillary column (HP5-MS, 30 m, 0.25 mm, 0.25 µm) was used. The initial oven temperature to hold at 50°C for 1 min, to rise to 200°C at 25°C /min and from 200°C to 300°C at 80°C /min and was held for 5.5 min. The injector ion source and quadrupole temperatures were 295°C, 300°C and 180°C, respectively. High purity helium (He) was used as the carrier gas at constant flow mode (1.5 mL/min, 45 cm/s linear velocity). The MSD to run in selected ion-monitoring mode. Compounds were identified on the basis of their retention times, target and qualifier ions. Qualification was based on the Internal Standard Calibration Procedure.

Polyphenols measurement was performed following the Standard Methods 5520 B [60] with a gas chromatography-mass spectrometry (GC-MS) (Hewlett-Packard 6980/HP5973MSD). Mass spectra were recorded using aVGTS 250 spectrometer equipped with a capillary SE 52 column (0.25 mm ID, 25 m) at 220°C with an isothermal program for 10 min. The total phenol was monitored as follows: 40 mL of TI ww was acidified to pH=2.0 by the addition of concentrated HCl. Phenols were then extracted with ethyl acetate. The organic phase was concentrated at 40°C to about 1 mL and silylized by the addition of N, O-bis(trimethylsilyl)acetamide (BSA). The resulting trimethylsilyl derivatives were analysed by GC-MS (Hewlett-Packard 6980/HP5973MSD).

Cerium Dioxide (CeO_2) Mechanism

Low-temperature hydrothermal synthesis is one method of making nanocrystalline CeO_2 particles [63]. Raw materials for this synthesis are cerium carbonate ($Ce_2(CO_3)3{\cdot}3H_2O$), hydrous cerium oxide, acetic acid (CH_3COOH), hydrogen peroxide (H_2O_2), nitrit acid (HNO_3) and ammonia (NH_3). When cerium (IV) hydroxide ($Ce(OH)_4$) is used as the precursor for CeO_2, $Ce_2(CO_3)_3{\cdot}3H_2O$ is first dissolved in HNO_3 to yield $Ce(NO_3)_2{\bullet}6H_2O$. $Ce(NO_3)_2{\bullet}6H_2O$ is diluted to 0.5 M Ce^{+4} using distilled H_2O. H_2O_2 in H_2O_2 / Ce^{+4}=1/2 molar ratio is added to $Ce(NO_3)_2{\bullet}6H_2O$ and stirred for 5 min under heat to convert Ce^{+3} to Ce^{+4}. Dilute 7 M NH_3 is then added to the mixture until pH=8.8. Upon

adding NH_3, $Ce(OH)_4$ or $CeO_2 + 2H_2O$ is precipitated with a light yellow color. The precipitate is washed with distilled H_2O several times, then placed in an oven to dehydrate at 250°C for 6 h and form CeO_2 particles [63].

Statistical Analysis

Analysis of variance (ANOVA) of experimental data was performed to determine the F and P values, i.e. the ANOVA test was used to test the differences between dependent and independent groups [64]. Comparison between the actual variation in experimental data averages and standard deviation was expressed in terms of F ratio. F was equal to 'found variation of the data averages/expected variation of the data averages'. P reports the significance level. Regression analysis was applied to the experimental data to determine the regression coefficient (R^2) [65].

All experiments were carried out three times and the results given as the means of triplicate samplings. Individual TI ww concentrations are given as the mean with Standard Deviation (SD) values.

Results and Discussions

Effect of sonication frequency on the COD_{dis} removals in TI ww

Three different sonication frequencies (25 kHz, 35 and 132 kHz) was researched under ambient conditions (25°C), at constant sonication power (640 W) and increasing sonication times (for 60 min, 120 and 150 min) to determine the optimum sonication frequency for maximum COD_{dis} removals in TI ww. Among the frequencies used in the sonication process (25 kHz, 35 and 132 kHz) it was found that a sonication frequency of 35 kHz is the optimum frequency for maximum COD_{dis} removals in TI ww (Table 6).

Sonication Frequency (kHz)	CODdis Removal Efficiencies in TI ww (%)		
	60 min	120 min	150 min
25	26.40	45.39	69.11
35	30.43	53.69	74.27
132	28.31	51.56	73.07

Table 6: Effect of sonication frequency on the COD_{dis} removals in TI ww at ambient conditions (25oC) (sonication power=640 W, sonication times=60 min, 120 and 150 min, initial COD_{dis} concentration in TI ww=962.99 mg/L, n=3, mean values).

Effect of sonication power on the COD_{dis} removals in TI ww

120-350-640 and 3000 W different sonication powers was researched under ambient conditions (25°C), at constant sonication frequency (35 kHz) and increasing sonication times (for 60 min, 120 and 150 min) to determine the optimum sonication power for maximum COD_{dis} removals in TI ww. Among the powers used in the sonication process (120-350-640 and 3000 W) it was found that a sonication power (640 W) is the optimum power for maximum COD_{dis} removals in TI ww (Table 7).

Sonication Power (W)	CODdis Removal Efficiencies in TI ww (%)		
	60 min	120 min	150 min
120	9.14	15.30	22.47
350	17.66	29.08	40.54
640	30.43	53.69	74.27
3000	28.75	52.71	73.43

Table 7: Effect of sonication power on the COD_{dis} removals in TI ww at ambient conditions (25°C) (sonication frequency=35 kHz, sonication time=60 min, 120 and 150 min, initial COD_{dis} concentration in TI ww=962.99 mg/L, n=3, mean values).

In general, when ultrasonic irradiation is used, the degradation ratio gradually becomes higher when the output power of the ultrasound is increased from 120 W to 640 W. The sono-degradation of pollutants increased with increasing applied power. As the power increased, the number of collapsing cavities also increased, thus leading to enhanced degradation rates, as reported by Busetti et al. [66], Papadaki et al. [67] and Psillakis et al. [68,69]. The vibration of sound in the cavitation area was increased with increasing applied power. More cavitation bubbles were produced during increasing applied power. However, the lifetime of this cavitation bubbles are shorter than the lifetime of cavitation bubbles at increasing power compared to a medium power. Thus resulting in low $OH^{\bullet}$ production and COD removals.

Effect of sonication time on the CODdis removals in TI ww

5-10-15-20-25-30-35-40-45-50-55-60-120 and 150 min sonication times was researched under ambient conditions (25°C), at constant sonication frequency (35 kHz) and constant sonication power (640 W) to determine the optimum sonication time for maximum COD_{dis} removals in TI ww. Among the sonication times used in the sonication process (0-60-120 and 150 min) it was found that 150 min sonication time is the optimum sonication time for maximum COD_{dis} removals in TI ww (Table 8).

Sonication Time (min)	CODdis Removal Efficiencies in TI ww (%)
0	0.00
5	2.32
10	4.07
15	6.80
20	8.44
25	9.67
30	10.29
35	13.65
40	17.15
45	20.81
50	24.33
55	28.01
60	30.43
120	53.69
150	74.27

Table 8: Effect of sonication time on the COD_{dis} removals in TI ww at ambient conditions (25°C) (sonication frequency=35 kHz, sonication power=640 W, initial COD_{dis} concentration in TI ww=962.99 mg/L, n=3, mean values).

Higher sonication times are needed for complete mineralization. Short sonication times did not provide high degradation yields for COD_{dis} since they were not exposed for a long enough time to ultrasonic irradiation. Moreover, the degradation of COD_{dis} under sonication which ultimately is expected to alter the effectiveness of ultrasonic extractions at long sonication times. The cavities are more readily formed when using solvents with low viscosity and low surface tension during long sonication times [70,71]. Among the solvents used acetone and hexane have the highest surface tension and viscosity. The preliminary studies showed that solvents with high surface ten-

sion and viscosity generally have a higher threshold for cavitation resulting in fewer cavitation bubbles but more harsh conditions once cavitation is established resulting in higher temperatures and pressures upon bubble collapse [72]. Higher vapor pressure leads to more solvent volatilizing into cavitation bubbles which are able to be dissociated by high temperature after 150 min sonication. Hexane and acetone have the highest vapor pressure among solvents. Thus, more hexane molecules migrate into cavitation bubbles leading to more molecules dissociating to generate radicals.

Effect of sonication volume on the COD_{dis} removals in TI ww

25-50-100-150-250-500 and 1000 mL different sonication volumes was researched under ambient conditions (25°C), at constant sonication frequency (35 kHz), constant sonication power (640 W) and increasing sonication times (for 60 min, 120 and 150 min) to determine the optimum sonication volume for maximum COD_{dis} removals in TI ww. Among the sonication volumes used in the sonication process (25-50-100-150-250-500 and 1000 mL) it was found that the COD_{dis} yields are close to each other in volumes of 50-100-150-250-500 and 1000 mL. However, the optimum sonication volume for maximum COD_{dis} removals in TI ww was recorded as 500 ml. A significant correlation between yields and sonication volumes was obtained (ANOVA, F=12.67, F=14.88, F=15.78, R^2=0.83, R^2=0.84, R^2=0.84, p=0.05 for TI ww) (Table 9).

Sonication Volume (mL)	COD_{dis} Removal Efficiencies in TI ww (%)		
	60 min	120 min	150 min
25	24.26	49.38	73.82
50	25.10	50.61	73.64
100	27.54	51.49	74.57
150	28.33	52.48	74.46
250	29.27	53.14	73.93
500	30.43	53.69	74.27
1000	28.48	53.50	72.36

Table 9: Effect of sonication volume on the COD_{dis} removals in TI ww at ambient conditions (25°C) (sonication frequency=35 kHz, sonication power=640 W, sonication time=60 min, 120 and 150 min, initial COD_{dis} concentration in TI ww=962.99 mg/L, n=3, mean values).

In this study, even if the difference between the seven volumes is very big, there is a slight decrease of sono-degradation yields of COD_{dis} yields in TI ww samples, respectively, at high volumes. The main reason for this effect may be the homogeneous agitation given both by magnetic stirring and the sonication waves. Under these conditions, the wastewater move homogenous to the most active sonication zone. Some studies showed that when the volume gets larger, the solution cannot be mixed as effectively as in a smaller volume and the wastewater cannot move to the most active sonication zone:

David [73] mentioned that the volume of the solution should be kept as small as possible, depending on the affective volume of sonicator in order to keep the solution in homogeneous turbulence throughout sonication. Kidak et al. [74] determined that when the volume gets larger, the solution cannot be mixed as effectively as in a smaller volume and sonication yields dereased. In our study, the maximum COD_{dis} removal efficiencies were observed at 500 mL sonication volume. COD_{dis} removal efficiencies were not significantly varied between 25 and 500 mL sonication volumes. Significant correlations between COD_{dis} yields and sonication volumes was not observed (R^2=0.48, R^2=0.43, R^2=0.37, F=3.45, F=2.78, F=3.78, p=0.05 for TI ww). Therefore, the sono-degradation rates of pollutants were accelerated with active reactive radicals ($O^•$, $OH^•$, $OOH^•$…etc.) in cavitation solution at long (150 min) sonication times.

Increasing the sonication frequency did not increase the number of free radicals, therefore a low number of free radicals did not escape from the bubbles and did not migrate [73]. Explanation of such phenomenon is not yet fully understood, since a more energetic implosion of cavitation bubbles is expected to occur at low frequency rather than at high frequency because of a larger bubbles radius observed at low frequency [75,76]. According to Minnaert [77], the size of bubbles formed in water, under one atmosphere, is inversely proportional to the frequency of the wave [78,79]. However, the larger the bubble size, the greater the water vapour within the bubble, leading to a more important damping of the collapse at low frequency like 20-40 kHz 73]. This damping induces a decreases in the temperature and pressure within the cavitation bubble at low frequency compared to a medium frequency [78].

Effect of sonication temperature on the COD_{dis} removals in TI ww

25°C, 30 and 60°C sonication temperatures was researched at constant sonication frequency (35 kHz), constant sonication power (640 W) and increasing sonication times (for 60 min, 120 to 150 min) to determine the optimum sonication temperatures for maximum COD_{dis} removals in TI ww. Among the sonication temperatures used in the sonication process (25°C, 30 and 60°C) it was found that 30°C and 60°C sonication temperatures are the optimum sonication temperatures for maximum COD_{dis} removals in TI ww (Table 10).

Sonication Temperature (°C)	COD_{dis} Removal Efficiencies in TI ww (%)		
	60 min	120 min	150 min
25	30.43	53.69	74.27
30	42.39	67.34	81.53
60	48.08	64.48	84.92

Table 10: Effect of sonication temperature on the COD_{dis} removals in TI ww (sonication frequency=35 kHz, sonication power=640 W, sonication time= 60 min, 120 and 150 min, initial COD_{dis} concentration in TI ww=962.99 mg/L, n=3, mean values).

Increased temperatures most likely facilitated bubble formation due to an increase of the equilibrium vapor pressure. This beneficial effect was compensated by the fact that bubbles contained more vapor and consequently reduced the maximum temperature obtained during bubble collapse. Furthermore, increased temperatures probably encouraged degassing of the liquid phase, thus reducing the number of gas nuclei available for bubble formation and the destruction rate of pollutants increased [69]. Furthermore, increased solution temperature allows molecules to move faster into the cavitation bubble (i.e., increase diffusivity) [80]. At higher temperatures more molecules will benefit from the temperature enhanced diffusivity and this may result in increase in removal rates for COD_{dis} at long sonication times [81].

Effect of sonication frequency and power on the degradation of TI ww

The effect of the ultrasonic frequency on the degradation ratio of COD_{dis} was also considered in the range from 35 kHz to 150 kHz. Increasing the sonication frequency did not increase the number of free radicals, therefore, a low number of free radicals did not escape

from the bubbles and did not migrate as reported by David [73]. The optimum time to reach equilibrium and the faster rate of removal in the presence of US was attributed to the higher mass transfer and higher surface area produced by the cavitation process [82]. The phenomenon responsible for removal of COD_{dis} is the formation of $OH^{\bullet}$ during sonication of aqueous solution by the cavitation process. This process consists of the formation, growth and collapse by violent implosions to release extreme temperatures and pressures at local hot spots $_{in}$ the liquid [83]. Under these critical conditions, the entrapped molecules of H_2O in the bubble dissociate into very reactive $OH^{\bullet}$ and $H^{\bullet}$ [84]. 61% maximum COD_{dis} removal was observed after 150 min sonication time, at 25°C, at 35 kHz US frequency, at 640 W sonication power, at 2.14 W/mL power density, at 51.4 W/cm^2 US intensity, at 11.5 kWh/kg $COD_{influent}$ specific energy, at 40.69 cm^2 active acoustical vibration area and at 7.2 cm reactor diameters, respectively. The maximum COD_{dis} removal efficiency of our other studies such as petrochemical industry wastewaters (PCI ww) and olive mill industry wastewaters (OMW) was obtained at the same operational conditions at 25°C, after 150 min sonication time, at 35 kHz US frequency, at 640 W sonication power, at 2.14 W/mL power density, at 51.4 W/cm^2 US intensity, at 11.5 kWh/kg CODinfluent specific energy, at 40.69 cm^2 active acoustical vibration area and at 7.2 cm reactor diameters, respectively [85-93]. As the power increased, the number of collapsing cavities also increased, thus leading to enhanced degradation rates, as reported by Papadaki et al. [67] and Psillakis et al. [69].

Effect of increasing sonication time on the COD_{dis}, color and polyphenols removal efficiencies in ambient conditions (25°C)

TI ww samples were treated with sonicator at different sonication times (120 and 150 min) at 25°C ambient conditions (Figure 2a; Table 11, SET 1). 53.69% and 74.27% COD_{dis} removals were observed at 120 and 150 min sonication time, respectively, at pH=7.0 and at 25°C (Figure 2a; Table 11, SET 1). The maximum COD_{dis} removals was 74.27% after 150 min sonication time, at pH=7.0 and at 25°C. As the sonication time was increased the COD_{dis} removal efficiency in TI ww was enhanced. A significant linear correlation between COD_{dis} yields and sonication time was observed (R^2=0.74, F=11.90, p=0.01) (Figure 2a; Table 11, SET 1). The optimum time to reach equilibrium and the faster rate of removal in the presence of US was attributed to the higher mass transfer and higher surface area produced by the cavitation process [82]. The phenomenon responsible for removals of COD_{dis} is the formation of $OH^{\bullet}$ during sonication of aqueous solution by the cavitation process [83]. This process consists of the formation, growth and collapse by violent implosions to release extreme temperatures and pressures at local hot spots in the liquid [83]. Under these critical conditions, the entrapped molecules of H_2O in the bubble dissociate into very reactive $OH^{\bullet}$ and hydrogen radicals ($H^{\bullet}$) [84]. He et al. [94] 70% COD removal found in a TI ww containing 20 mg/L C.I. Reactive Blue 19, at 20 kHz, at 176 W, at 176 W/L, after 30 min sonication time, at 30°C and at pH=8.0. In this study, 74.27% COD_{dis} removal was observed after 150 min sonication time and at 25°C. The COD_{dis} yield in the present study is higher than the yield obtained by The et al. [94] at 30°C and at a pH of 8.0.

53.47% and 57.09% color removals were found after 120 and 150 min sonication time, respectively, at pH=7.0 and at 25°C (Figure 2b; Table 12, SET 1). The maximum color removal efficiency was 57.09% after 150 min sonication time, at pH=7.0 and at 25°C. A significant linear correlation between color yields and sonication time

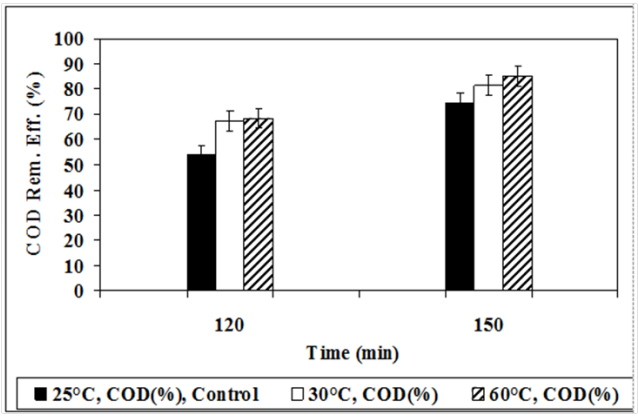

Figure 2a: Effect of increasing temperature on the a) COD_{dis} and b) color removal efficiencies in TI ww versus increasing sonication times (sonication power=640 W, sonication frequency=35 kHz, initial COD_{dis} concentration=962.99 mg/L, initial color concentration=88.56 1/m, n=3, mean values).

was obtained (R^2=0.83, F=10.92, p=0.01) (Figure 2b; Table 12, SET 1). The main reaction pathway for TI ww containing azo dye solutions is the oxidation by $OH^{\bullet}$ attack in the bulk liquid via sonication in Equation (5), while thermal reactions may occur at the bubble-liquid interface for some dye molecules to approach gaseous bubble surfaces as reported by Ince and Tezcanli-Guyer [95] in Equation (6):

$$OH^{\bullet} + Dye \rightarrow [Dye\text{–}OH\ addic]^{\bullet} \rightarrow Oxidized\ dye + CO_2 + H_2O \quad (5)$$

$$Dye \xrightarrow{)))} Organic\ radicals + Dissociated\ dye\ fragments + C_2H_4 \quad (6)$$

Methylene Blue and Rhodamine B dyestuffs were selected for our study. It is expected that the sonolytic degradation of Methylene Blue and Rhodamine B dyestuffs would mainly occur by OHl attack [96,97]. In order to investigate the dependence of the $OH^{\bullet}$ during the degradation of Methylene Blue and Rhodamine B dyestuffs by ultrasonic irradiation, the sonolytic degradation of Methylene Blue and Rhodamine B in the presence of radical scavengers (such as $H^{\bullet}$, $OH^{\bullet}$, $O_2H^{\bullet}$, $O2^{\bullet}$), known as an effective $OH^{\bullet}$ scavenger, was performed and was to scavenge $OH^{\bullet}$ in the bubble and prevent the accumulation of $OH^{\bullet}$ at the interface of the bubble [96,97]. After the decolorization, the process could shift progressively from the bulk solution to the surface of the catalysts and cleavage of the carbon (C), hydrogen (H_2) and oxygen (O_2) rings was mainly attributed to the radical scavengers (H•, OH•, O_2H•, O_2•) reactions. The organic dyes (acid, basic, direct, reactive, vat, etc.) are totally mineralized to simple inorganic species such as CO_3^-, Cl^- and NO_3^- [98]. Vankar and Shanker [99] found that the ultrasonic waves can reduce the concentration of Methylene Blue up to 10% in 30 min sonication time and at 30°C. In this study, 57.09% color removal was observed after 150 min sonication time and at 25°C. The color yield in the present study is higher than the yield obtained by Vankar and Shanker [99] at 30°C.

Total phenol (PHE R) and three polyphenols [4-methyl phenol (C_7H_8O) (4-MP), 4-hydroxyanisole ($C_7H_8O_2$) (4-H), 2-methyl-4-hydroxyanisole ($C_8H_{10}O_2$) (2-M-4-H)] were measured in TI ww during sonication process after 120 and 150 min sonication time. 55% PHE R, 45% 4-MP, 42% 4-H and 40% 2-M-4-H polyphenols removals were measured after 120 min sonication time, respectively, at pH=7.0 and at 25°C (Table 13). 70% PHE R, 65% 4-MP, 64% 4-H and 60% 2-M-4-H polyphenols removals were observed after 150 min sonication time, respectively, at pH=7.0 and at 25°C. The maximum polyphenols removals were 70% PHE R, 65% 4-MP, 64% 4-H and 60%

No	Parameters	COD_{dis} Removal Efficiencies (%)					
		25oC					
		0. Min		120. min		150. min	
1	Raw ww, control	0		53.69		74.27	
		30oC			60oC		
		0. min	120. min	150. min	0. min	120. min	150. min
2	Raw ww, control	0	67.34	81.53	0	68.48	84.92
3	nano-CeO2=10 mg/L	0	59.47	81.24	0	72.03	86.41
	nano-CeO2=100 mg/L	0	66.65	85.10	0	84.05	90.64
	nano-CeO2=1000 mg/L	0	79.87	90.22	0	87.17	96.70
4	nano-TiO2=0.5 mg/L	0	68.94	83.43	0	74.43	89.20
	nano-TiO2=10 mg/L	0	71.15	89.27	0	82.22	91.17
	nano-TiO2=20 mg/L	0	75.75	94.11	0	85.60	98.13
5	nano-CeO2/TiO2=100 mg/L	0	70.00	88.41	0	72.90	91.18
	nano-CeO2/TiO2=500 mg/L	0	75.22	92.15	0	78.08	97.20
	nano-CeO2/TiO2=1000 mg/L	0	84.51	97.39	0	89.24	99.37

Table 11: COD_{dis} removal efficiencies of TI ww before and after sonication with the addition of different nano-CeO_2, nano-TiO_2 and nano-CeO_2/TiO_2 concentrations, at initial COD_{dis} concentrations=962,99 mg/L, at sonication power=640 W and at sonication frequency=35 kHz (n=3, mean values).

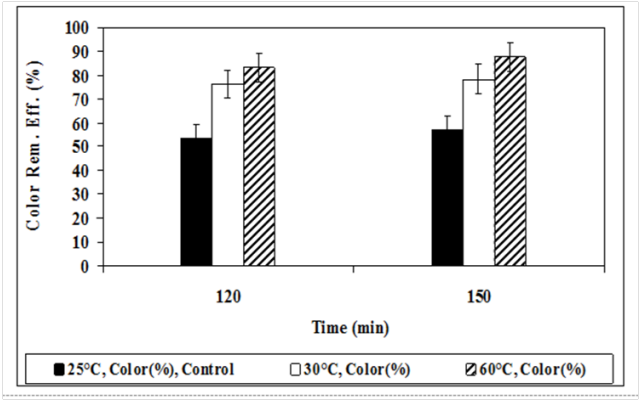

Figure 2b: Effect of increasing temperature on the a) COD_{dis} and b) color removal efficiencies in TI ww versus increasing sonication times (sonication power=640 W, sonication frequency=35 kHz, initial COD_{dis} concentration=962.99 mg/L, initial color concentration=88.56 1/m, n=3, mean values).

2-M-4-H after 150 min sonication time, respectively, at pH=7.0 and at 25°C. A significant linear correlation between polyphenols removals and sonication time was observed (R^2=0.88, F=15.64, p=0.01) (Table 13). Pyrolytic destruction of the polyphenols in the gas phase is negligible; the degradation occurs mainly in the bulk solution. A possible explanation for this is that a considerable increase in the concentration results in the formation of a complex H-bonding network between the polyphenolic compounds [100]. During sonication low decrease of total phenol concentrations in the effluent samples results in the formation of a complex H-bonding network betw een the polyphenolic compounds after 60 min sonication time. It is well known that molecules containing COOH or CHO groups exist as dimmers in solution due to the formation of H-bonds between two neighboring molecules. This results in a more robust and stable configuration, thus leading to reduced degradation [101]. In addition to this, the formation of such a network may impede their diffusion towards the bubble interface and this would also lead to reduced degradation of polyphenols [102].

Effect of increasing temperature on the removal of COD_{dis}, color and polyphenols versus sonication time

67.34% and 81.53% COD_{dis} removals were observed after 120 and 150 min sonication time, respectively, at pH=7.0 and at 30°C (Figure 2a; Table 11, SET 2). 13.65% and 7.26% increase in COD_{dis} removals were obtained after 120 and 150 min sonication time, respectively, at pH=7.0 and at 30°C, compared to the control (E=74.27% COD_{dis} after 150 min sonication time at pH=7.0 and at 25°C). A significant linear correlation between COD_{dis} yields and temperature was not observed (R^2=0.33, F=2.88, p=0.01) (Figure 2a; Table 11, SET 2). 68.48% and 84.92% COD_{dis} yields were found after 120 and 150 min sonication time, respectively, at pH=7.0 and at 60°C (Figure 2a; Table 11, SET 2). The contribution of temperature on COD_{dis} removals were 4.79% and 10.65% after 120 and 150 min sonication time, respectively, at pH=7.0 and at 60°C, compared to the control (E=74.27% COD_{dis} after 150 min sonication time, at pH=7.0 and at 25°C). The maximum COD_{dis} removal was 84.92% after 150 min sonication time at pH=7.0 and at 60°C. A significant linear correlation between COD_{dis} yields and temperature was observed (R^2=0.71, F=13.92, p=0.01) (Figure 2a; Table 11, SET 2). With an increase in the temperature, the initial sono-degradation rate was increased in TI ww [103]. This could be explained by the hydrophilic property of the pollutant which is mostly degraded outside the cavitation process by the $OH^{\bullet}$ produced by US in TI ww [103]. Therefore, reactions in the bulk are facilitated by increasing the temperature due to the higher mass transfer of different species at higher temperatures and this leads to an enhancement of the reaction rate of radicals with COD molecule [104]. On the other hand, any increase in temperature will raise the vapor pressure of a medium and so lead to easier cavitation [105,106].76.38% and 78.26% color removals were observed after 120 and 150 min sonication time, respectively, at pH=7.0 and at 30°C (Figure 2b; Table 12, SET 2).

No	Parameters	Color Removal Efficiencies (%)					
		25°C					
		0. Min		120. min		150. min	
1	Raw ww, control	0		53.47		57.09	
		30°C			60°C		
		0. min	120. min	150. min	0. min	120. min	150. min
2	Raw ww, control	0	76.38	78.26	0	83.20	87.66
3	nano-CeO_2=10 mg/L	0	77.79	80.96	0	85.08	88.54
	nano-CeO_2=100 mg/L	0	78.61	82.14	0	86.37	89.19
	nano-CeO_2=1000 mg/L	0	80.73	83.78	0	91.07	95.06
4	nano-TiO_2=0.5 mg/L	0	79.67	84.14	0	85.78	91.19
	nano-TiO_2=10 mg/L	0	82.84	88.60	0	88.60	94.95
	nano-TiO_2=20 mg/L	0	83.78	90.13	0	90.83	96.24
5	nano-CeO_2/TiO_2=100 mg/L	0	87.31	89.31	0	88.95	91.42
	nano-CeO_2/TiO_2=500 mg/L	0	88.37	91.07	0	90.60	95.89
	nano-CeO_2/TiO_2=1000 mg/L	0	89.31	93.42	0	91.30	98.07

Table 12: Color removal efficiencies of TI ww before and after sonication with the addition of different nano-CeO_2, nano-TiO_2 and nano-CeO_2/TiO_2 concentrations, at initial color concentrations=88.56 1/m, at sonication power=640 W and at sonication frequency=35 kHz (n=3, mean values).

Time (min)	PHE0 (mg/L)	25°C, control						
		PHE R (%)	4-MP (mg/L)	4-MP R (%)	4-H (mg/L)	4-H R (%)	2-M-4-H (mg/L)	2-M-4-H R (%)
0	37	0	0	0	0	0	0	0
120								
120	16.65	55	5.20	45	8.52	42	10.11	40
150	11.10	70	3.31	65	5.29	64	6.74	60
Time (min)	PHE0 mg/L)	30°C						
		PHE R (%)	4-MP (mg/L)	4-MP R (%)	4-H (mg/L)	4-H R (%)	2-M-4-H (mg/L)	2-M-4-H R (%)
0	37	0	0	0	0	0	0	0
120	15.17	59	5	50	8.40	48	9.78	46
150	8.14	78	2.50	75	4.85	70	6.34	65
Time (min)	PHE0 (mg/L)	60°C						
		PHE R (%)	4-MP (mg/L)	4-MP R (%)	4-H (mg/L)	4-H R (%)	2-M-4-H (mg/L)	2-M-4-H R (%)
0	37	0	0	0	0	0	0	0
120	12.58	66	4.85	55	8.20	51	8.54	49
150	5.55	85	2.26	79	4.35	74	4.69	72

Table 13: Measurements of total phenols and three polyphenols (4-methyl phenol, 4-hydorxyanisole and 2-methyl-4-hyroxyanisole) in TI ww with GC-MS after 120 and 150 min sonication time, at pH=7, at increasing temperatures, at initial total phenol concentration=37 mg/L, at sonication power=640 W and at sonication frequency=35 kHz (n=3, mean values).

PHE0: Initial total phenol concentration (mg/L), PHE R: Total phenol removal efficiency (%), 4-MP: 4-methyl phenol concentration after sonication (mg/L), 4-MP R: 4-methyl phenol removal efficiency (%), 4-H: 4-hydorxyanisole concentration after sonication (mg/L), 4-H R: 4-hydorxyanisole removal efficiency (%), 2-M-4-H: 2-methyl-4-hyroxyanisole concentration after sonication (mg/L), 2-M-4-H R: 2-methyl-4-hyroxyanisole removal efficiency (%).

22.91% and 21.17% increase in the color removals were obtained after 120 and 150 min sonication time, respectively, at pH=7.0 and at 30°C, compared to the control (E=53.47% and E=57.09% color after 120 and 150 min sonication time, respectively, at pH=7.0 and at 25°C). A significant linear correlation between color yields and temperature was not observed (R^2=0.46, F=4.51, p=0.01 (Figure 2b; Table 12, SET 2). 83.20% and 87.66% color yields were found after 120 and 150 min sonication time, respectively, at pH=7.0 and at 60oC (Figure 2b; Table 12, SET 2). The contribution of temperatures on color removals were 29.73% and 30.57% after 120 and 150 min sonication time, respectively, at pH=7.0 and at 60°C, compared to the control (E=53.47% and E=57.09% color after 120 and 150 min son-

ication time, respecvtively, at pH=7.0 and at 25°C). The maximum color removal was 87.66% after 150 min sonication time at pH=7.0 and at 60°C. A significant linear correlation between color yields and temperature was not observed (R^2=0.51, F=3.09, p=0.01) (Figure 2b; Table 12, SET 2). Sayan [107] reported 80.62% color removal in a TI ww containing 1000 mg/L Rifacion Yellow HE4R with US and combined US/activated carbon at 850 kHz, at 140 W, after 120 min sonication time and at 30°C. In this study, 78.26% color removal was observed after 150 min sonication time and at 30°C. In this study, similar yields were observed with the yields obtained by Sayan [107] at 30°C as mentioned above. 78% PHE R, 75% 4-MP, 70% 4-H and 65% 2-M-4-H polyphenols removals were observed after 150 min sonication time, respectively, at pH=7.0 and at 30oC (Table 13). 8% PHE R, 10% 4-MP, 6% 4-H and 5% 2-M-4-H increase in polyphenols removals were obtained after 150 min sonication time, respectively, at pH=7.0 and at 30°C, compared to the control (E=70% PHE R, E=65% 4-MP, E=64% 4-H, E=60% 2-M-4-H polyphenols after 150 min sonication time, at pH=6.98 and at 25°C). A significant linear correlation between polyphenols yields and temperature was observed (R^2=0.83, F=13.95, p=0.01) (Table 13). 85% PHE R, 79% 4-MP, 74% 4-H and 72% 2-M-4-H polyphenols yields were found after 150 min sonication time, respectively, at pH=7.0 and at 60°C (Table 13). The contribution of temperatures on polyphenols removals were 15%, 14%, 10% and 12% for PHE R, 4-MP, 4-H and 2-M-4-H, respectively, after 150 min sonication time, respectively, at pH=7.0 and at 60°C, compared to the control (E=70% PHE R, E=65% 4-MP, E=64% 4-H, E=60% 2-M-4-H polyphenols after 150 min sonication time, at pH=6.98 and at 25°C). The maximum polyphenols removals were 85% PHE R, 79% 4-MP, 74% 4-H and 72% 2-M-4-H after 150 min sonication time, respectively, at pH=7.0 and at 60°C. A significant linear correlation between polyphenols removals and temperature was obtained (R2=0.87, F=14.70, p=0.01) (Table 13). The degradation of phenol occurs in the bulk liquid medium due to hydroxylation reaction induced by $OH^{\bullet}$ generated from cavitation bubble [108]. This is a consequence of low vapor pressure of phenol (due to which it does not evaporate into the cavitation bubble) and the hydrophilic nature of the phenol molecule. The interaction between radicals and phenol molecules becomes an important factor influencing the overall degradation. The scavenging phenomenon increases the sonodegradation of phenol. Moreover, the concentration of the radical scavenging species is another important factor affecting the degradation. The formation of $OH^{\bullet}$ and H_2 derived from sonolysis of H_2O in aqueous solution saturated with O_2 as an endpoint of inertial cavitation was examined. It should be pointed out that $OH^{\bullet}$, formed via H_2O sonolysis, can partly recombine yielding H_2O_2 which in turn reacts with H_2 to regenerate $OH^{\bullet}$ in Equations (7) and (8) [108]:

$$OH^{\bullet} + OH^{\bullet} \Leftrightarrow H_2O_2 \quad (7)$$

$$H_2O_2 + H^{\bullet} \rightarrow H_2O + OH^{\bullet} \quad (8)$$

Takizawa et al. [109] found that US-assisted the hydroxylation of phenolic compounds, such as phenol, 4-methyl phenol, 4-hydroxyanisole, 2-naphthol, catechol, resorcinol, 3-t-butyl-4-hydroxyanisole, 3-methyl-4-hydroxyanisole, in aqueous solution in 12-18 h, at 200 kHz. In the present study, we agree with the results of Takizawa et al. [109] in TI ww.

Effect of nano-cerium dioxide (nano-CeO_2) concentrations on the COD_{dis}, color and polyphenols removal efficiencies versus sonication time and temperature

81.24%, 85.1% and 90.22% COD_{dis} removals were observed in 10, 100 and 1000 mg/L nano-CeO_2, respectively, after 150 min sonication time at pH=7.0 and at 30°C (Table 11, SET 2 and SET 3). 3.69%, 6.59% and 13.57% increase in COD_{dis} removals were obtained in 10, 100 and 1000 mg/L nano-CeO_2, respectively, after 150 min sonication time at pH=7.0 and at 30°C, compared to the control (without nano-CeO_2 while E=81.53% COD_{dis} at pH=7.0 and at 30°C, after 150 min sonication time). A significant linear correlation between COD_{dis} yields and increasing nano-CeO_2 concentrations was observed (R^2=0.86, F=14.12, p=0.01) (Table 11, SET 2 and SET 3). 86.41%, 90.64% and 96.70% COD_{dis} yields were found in 10, 100 and 1000 mg/L nano-CeO^2, respectively, after 150 min sonication time, at pH=7.0 and at 60°C (Table 11, SET 2 and SET 3). The contribution of nano-CeO^2 on COD_{dis} removals were 2.50%, 8.70% and 13% in 10, 100 and 1000 mg/L nano-CeO_2, respectively, after 150 min sonication time, at pH=7.0 and at 60°C, compared to the control (E=84.92% COD_{dis} after 150 min sonication time, at pH=7.0 and at 60°C). The maximum COD_{dis} removal was 96.70% at nano-CeO_2=1000 mg/L after 150 min sonication time, at pH=7.0 and at 60°C. A significant linear correlation between COD_{dis} yields and increasing nano-CeO_2 concentrations was observed (R^2=0.92, F=16.43, p=0.01) (Table 11, SET 2 and SET 3). A simple scheme showing radical formation and depletion during H_2O sonolysis is given below in Equations (9), (10), (11) and (12) [110]:

$$H_2O \rightarrow))) OH^{\bullet} + H^{\bullet} \ (pyrolysis) \quad (9)$$

$$OH^{\bullet} + H^{\bullet} \rightarrow H_2O \quad (10)$$

$$2\,OH^{\bullet} \rightarrow H_2O + O^{\bullet} \quad (11)$$

$$2\,OH^{\bullet} \rightarrow H_2O_2 \quad (12)$$

Cerium (Ce) is quite electropositive and reacts slowly with H_2O and quite quickly with hot H_2O to form $Ce(OH)_3$ in Equation (13). Ce^{+4} ions is reacted with OH- ions and is converted $Ce(OH)_4$ in Equation (14). $Ce(OH)_4$ is reduced to CeO_2 and H_2O in Equation (15) [111]:

$$2\,Ce(s) + 6\,H_2O(l) \rightarrow 2\,Ce(OH)_3(aq) + 3H_2(g) \quad (13)$$

$$Ce^{+4} + 4OH^{-} \rightarrow Ce(OH)_4 \quad (14)$$

$$Ce(OH)_4 \rightarrow CeO_2 + 2\,H_2O \quad (15)$$

Oxides of rare earth elements have been used widely in the catalyst industry to improve activity, selectivity and thermal stability. CeO_2 is one of the most significant of these rare earth elements and has seen recent use as a catalyst. The catalyst function of CeO_2 is related to its gas phase reaction with O_2 and ability to shift between the reduced and oxidized state, i.e., Ce^{+3} and Ce^{+4} ions. This reversible reaction is expressed in Equation (16) [111]:

$$CeO_2 \rightarrow CeO_{2-x} + (x/2)\,O_2 \quad (x = 0\ or\ 0.5) \quad (16)$$

The mechanism of catalytic activity on CeO_2 is a complicate [112]. The revolve of the O_2 storage capacity which is largely due to the multivalent nature of Ce at the surface of the pollutant materials change in energy for any heterogeneous catalyst in the surface. The shift between the Ce^{+3} to Ce^{+4} states leads to a high O_2 mobility in CeO_2 lattice, which in turn can lead to a strong catalytic potential. The morphological analysis confirms the formation of CeO_2 NPs [113]. Ac impedance spectroscopy has been used to study the ion conduction and conductivity of the prepared NPs without sonication and with 1 h, 2 h, 3 h, and 4 h sonication time, at 350°C, at 380°C and at 410°C. After 2 h sonication time is found a high ionic conductivity (2.75 * 10-4 S/cm at 410°C) in the surface of the CeO_2. The conductance spectra show an orderly shifting which is due to the effect of sonication [113]. High ion conductivity increases to radical scavengers rate and also, high removal efficiencies of pollution compounds (COD, color, phenols, TAAs, etc.) during sonication process. Although, high ion conductivity decreases to sonication time during sonication process.

80.96%, 82.14% and 83.78% color removals were observed in 10, 100 and 1000 mg/L nano-CeO_2, respectively, after 150 min sonication time, at pH=7.0 and at 30°C (Table 12, SET 3). 2.70%, 3.88% and 5.52% increase in the color yields were obtained in 10, 100 and 1000 mg/L nano-CeO_2, respectively, after 150 min sonication time, at pH=7.0 and at 30°C, compared to the control (E=78.26% color, after 150 min sonication time, at pH=7.0 and at 30°C). A significant linear correlation between color yields and increasing nano-CeO_2 concentrations was observed (R^2=0.83, F=12.11, p=0.01) (Table 12, SET 2 and SET 3). 88.54%, 89.19% and 95.06% color yields were found in 10, 100 and 1000 mg/L nano-CeO_2, respectively, after 150 min sonication time, at pH=7.0 and at 60°C (Table 12, SET 3). The contribution of nano-CeO_2 concentrations on color removals were 0.88%, 1.53% and 7.4% in 10, 100 and 1000 mg/L nano-CeO_2, respectively, after 150 min sonication time, at pH=7.0 and at 60°C, compared to the control (E=87.66% color after 150 min sonication time, at pH=7.0 and at 60°C). 95.06% maximum color removal was observed in 1000 mg/L nano-CeO_2 after 150 min sonication time at pH=7.0 and at 60°C. A significant linear correlation between color yields and increasing nano-CeO_2 concentrations was observed (R^2=0.87, F=14.70, p=0.01) (Table 12, SET 2 and SET 3). Although, the color yields increased as the nano-CeO_2 concentrations, sonication time and sonication temperature were increased during sonication process. Li et al. [114] found that the disappearance of color occurred more readily than COD reduction for nano-CeO_2 catalysts. Dye chemicals are usually composed of molecules with large molecular structures. When the chromophore on the dye structure is degraded the color will disappear. Oxidation and pyrolysis are main degradation mechanisms for decolorization with the addition of CeO_2 at US system. Reactions in the bulk are facilitated by increasing the temperature due to the higher mass transfer of different species at higher temperatures and this leads to an enhancement of the reaction rate of radicals ($H^{\bullet}$, $OH^{\bullet}$, $O_2H^{\bullet}$) with dye molecules [114]. On the other hand, any increase in temperature will raise the vapor pressure of a medium and so lead to easier cavitation but less violent collapse [105,106].

Zhao et al. [115] performed the catalytic degradation of Rhodamine B and Safranin-T with MoO_3/CeO_2 NFs catalyst in a continuous flowing mode using air (O_2) as an oxidant. The results show that Rhodamine B and Safranin-T are degraded effectively with removal efficiencies of 98.30% and 98.50%, respectively. You et al. [116] observed the loading amount of CeO_2 and reaction temperature had important effects on decolorization ratio of Methyl Orange. At 70% loading amount and at 65°C reaction temperature, the decolorization ratio of Methyl Orange reached over 99%, which showed excellent catalytic activity. In this study, 95.06% color removal was found in nano-CeO_2=1000 mg/L after 150 min sonication time and at 60°C. The color yield in the present study is lower than the yield obtained by Zhao et al. [115] and by You et al. [116] at 65°C as mentioned above. This could be attributed to the differences between sonication temperature and dyestuff properties applied to the TI wws. Li et al. [117] investigated CeO_2-ZnO composite NFs applications in the treatment of organic-polluted water (TI ww). Photocatalytic activity experiments showed that the Rhodamine B was almost completely decomposed when it was catalyzed by CeO_2-ZnO NFs within 180 min, while only 17.40% and 82.30% Rhodamine B color removals were found with CeO_2 and ZnO NFs catalysis, respectively. Pradhan and Parida [10] 93% complete Methylene Blue photodegradation and complete Congo Red mineralization were observed. The reason for higher catalytic activity of 1/1 (Fe/Ce) is ascribed to their higher surface area, surface acidity which the active sites of the catalyst accelerates the photocatalytic reaction. In this study, 95.06% color removal was found in nano-CeO_2=1000 mg/L after 150 min sonication time and at 60°C. The color yields in the present study is higher than the yield obtained by Li et al. [117] at 60°C and by Pradhan and Parida [10] as mentioned above 80% PHE R, 73% 4-MP, 70% 4-H and 64% 2-M-4-H polyphenols removals were observed in nano-CeO_2=1000 mg/L after 150 min sonication time, respectively, at pH=7.0 and at 25°C (Table 14). 10% PHE R, 8% 4-MP, 6% 4-H and 4% 2-M-4-H increase in polyphenols removals were obtained in nano-CeO_2=1000 mg/L after 150 min sonication time, respectively, at pH=7.0 and at 25°C, compared to the control (E=70% PHE R, E=65% 4-MP, E=64% 4-H, E=60% 2-M-4-H polyphenols after 150 min sonication time, at pH=7.0 and at 25°C). A significant linear correlation between polyphenols yields and increasing nano-CeO_2 concentrations was observed (R2=0.87, F=16.49, p=0.01) (Table 13 and Table 14). 88% PHE R, 84% 4-MP, 78% 4-H and 71% 2-M-4-H polyphenols removals were observed in nano-CeO_2=1000 mg/L after 150 min sonication time, respectively, at pH=7.0 and at 30°C (Table 14). 10% PHE R, 9% 4-MP, 8% 4-H and 6% 2-M-4-H increase in polyphenols removals were obtained in nano-CeO_2=1000 mg/L after 150 min sonication time, respectively, at pH=7.0 and at 30°C, compared to the control (E=78% PHE R, E=75% 4-MP, E=70% 4-H and E=65% 2-M-4-H polyphenols after 150 min sonication time, at pH=7.0 and at 30°C). A significant.

Linear correlation between polyphenols yields and increasing nano-CeO_2 concentrations was found (R^2=0.88, F=16.32, p=0.01) (Table 14). 94% PHE R, 89% 4-MP, 83% 4-H and 80% 2-M-4-H polyphenols yields were found in nano-CeO_2=1000 mg/L after 150 min sonication time, respectively, at pH=7.0 and at 60°C (Table 14). 9% PHE R, 10% 4-MP, 9% 4-H and 8% 2-M-4-H increase in polyphenols removals were obtained in nano-CeO_2=1000 mg/L after 150 min sonication time, respectively, at pH=7.0 and at 60°C, compared to the control (E=85% PHE R, E=79% 4-MP, E=74% 4-H and E=72% 2-M-4-H polyphenols after 150 min sonication time, at pH=7.0 and at 60°C). The maximum polyphenols removals were 94% PHE R, 89% 4-MP, 83% 4-H and 80% 2-M-4-H in nano-CeO_2=1000 mg/L after 150 min sonication time, respectively, at pH=7.0 and at 60°C. A significant linear correlation between polyphenols yields and increasing nano-CeO_2 concentrations was obtained (R^2=0.75, F=14.11, p=0.01) (Table 14). Polyphenols mainly degrade by reacting with $OH^{\bullet}$ at the gas–liquid interface and/or in the bulk liquid and possibly to a much lesser ex-

tent by thermal decomposition at the gas-liquid interface [108]. Pradhan and Parida [10] investigated the nanostructured and mesoporous Fe-Ce mixed oxides for photocatalytic degradation of phenol. About 13% phenol sonodegradation. In this study, 80% PHE R removal was found in nano-CeO_2=1000 mg/L after 150 min sonication time and at 25°C. The total phenol yield in the present study is higher than the yield obtained by Pradhan and Parida [10] as mentioned above. This could be attributed to the differences between catalysis concentrations applied to the TI wws.

The degradation of pollutants in the photocatalytic process performed under UV or VIS irradiation depends on many parameters, including the pH of wastewater, effect of catalyst loading expressed by the ratio of catalyst to pollutant or catalyst to volume of wastewater, adsorption of a pollutant on a photocatalyst surface, source and light intensity, pollutant loading, and presence of interfering compounds [118,119].

The composition of industrial wastewater may vary, and some pollutants can poison photocatalysts and photoelectrocatalysts. Therefore, regeneration methods for CeO_2-based photocatalyst surfaces must be taken under consideration. Although there aremanyissues that should be overcome in photocatalytic and photoelectrocatalytic processes in wastewater treatment before these processes can be commercially implemented, CeO_2 and its composites seem to be promising photocatalytic materials [42].

Ceria containing materials has been receiving numerous attention recently owing to its broad ranges of application in catalysis [120-123] in ceramic materials [124,125] and in solid-oxide fuel cells [126,127]. With its use as an optical catalyst, CeO_2 displays a band gap of 3.2 eV electron transition from O 2p to Ce 4f [128]. CeO_2 is thus not generally considered as a semiconductor, nor is it regarded as a photoactive material. The recent work by Esch et al. [129] about the electron localization of CeO_2 observed by high-resolution scanning tunneling microscopy reveals the defect of CeO_2-being difficult to move, which means that the Ce^{+3}, or the electron trapped at 4f level cannot move at ambient temperatures. The results imply the inactive photocatalytic properties of CeO_2, i.e. the exciton produced by photoabsorption is difficult to move or diffuse to the surface and thus contributes little to its surface catalytic reaction. Research has been conducted to improve photocatalytic properties of CeO_2 powders by doping transition metal elements. With the nanoparticles doped, CeO_2 with 3d transition metal ions would enhance the mobility of exciton, thus facilitating its surface reaction. Accordingly, some transition metal ion dopants such as Fe, Mn, and Co have been investigated for the CeO_2 system.

The photocatalytic degradation of methylene blue (MB, $C_{16}H_{18}ClN_3S{\cdot}3H_2O$) is tested on the doped CeO_2 nanoparticles to check the dope effects. The doping of transition metal significantly enhances the photoactivity for MB reaction. Because the surface area of all the samples are approximately the same (the size of the doped CeO_2 nanoparticles is almost the same) and the energy of the Hg light used for the optical reaction is focused at the wavelengths shorter than 400 nm (365 nm 100%, 313 nm 20%, 254 nm 20%, and 410 nm 2%), it may be reasonable to attribute the improved photocatalytic activity of the doped ceria to the enhancement of energy transfer from the doping [130].

Effect of nano-titanium dioxide (nano-TiO_2) on the COD_{dis}, color and polyphenols removal 1efficiencies versus sonication time and temperature

83.43%, 89.27% and 94.11% COD_{dis} removals were observed in 0.5, 10 and 20 mg/L nano-TiO_2, respectively, after 150 min sonication time, at pH=7.0 and at 30oC (Table 11, SET 4). The contribution of these nano-TiO_2 concentrations on COD_{dis} yields were 1.90%, 7.74% and 12.58% compared to the control (without TiO_2 while E=81.53% COD_{dis} after 150 min sonication time, at pH=7.0 and at 30°C). A significant linear correlation between COD_{dis} yields and increasing nano-TiO_2 concentrations was observed (R^2=0.83, F=17.80, p=0.01) (Table 11, SET 4). 89.20%, 91.17% and 98.13% COD_{dis} yields were found in 0.5, 10 and 20 mg/L nano-TiO_2, respectively, after 150 min sonication time at pH=7.0 and at 60°C (Table 11, SET 4). The contribution of 0.5, 10 and 20 mg/L nano-TiO_2 concentrations on COD_{dis} removals were 4.28%, 6.25% and 13.21% compared to the control (without TiO_2 while E=84.92% COD_{dis} after 150 min sonication time, at pH=7.0 and at 60°C). The maximum COD_{dis} removal was 98.13% in nano-TiO_2=20 mg/L after 150 min sonication time, at pH=7.0 and at 60°C. A significant linear correlation between COD_{dis} yields and increasing nano-TiO_2 concentrations was observed (R^2=0.79, F=16.52, p=0.01) (Table 11, SET 4). Since the organic compounds in TI ww are hydrophilic, its partitioning into the gas phase is unlikely and direct pyrolysis should be a very minor reaction path in a TiO_2 with US process. Accordingly, the main pathway for the destruction of COD is chemical oxidation by $OH^{\bullet}$ in the bulk liquid and/or the interface region of the cavitation bubbles in the US-based system with the addition of different TiO_2 concentrations.

Since the organic compounds in TI ww are hydrophilic, its partitioning into the gas phase is unlikely and direct pyrolysis should be a very minor reaction path in a TiO_2/US system [57]. Accordingly, the main pathway for the destruction of COD is chemical oxidation by $OH^{\bullet}$ in the bulk liquid and/or the interface region of the cavitation bubbles in the US-based system [57].

In a study performed by Mrowetz et al. [56] 36% COD removal was found in a TI ww containing 75 mg/L Acid Orange 8, at 20 kHz, at 250 W, in TiO_2=0.1 g/L, after 100 min sonication time and at 35°C. In this study, 94.11% COD_{dis} removal was measured in nano-TiO_2=20 mg/L after 150 min sonication time and at 30°C. The COD_{dis} yield in the present study is higher than the yield observed by Mrowetz et al. [56] at 30°C as mentioned above. This could be attributed to the differences between dyestuff properties and nano-TiO_2 concentration applied to the TI wws. 84.14%, 88.60% and 90.13% color removals were observed in 0.5, 10 and 20 mg/L nano-TiO_2, respectively, after 150 min sonication time, at pH=7.0 and at 30°C (Table 12, SET 4). 5.88%, 10.34% and 11.87% increase in the color removals were obtained in 0.5, 10 and 20 mg/L nano-TiO_2, respectively, after 150 min sonication time, at pH=7.0 and at 30°C, compared to the control (without nano-TiO_2 while E=78.26% color, after 150 min sonication time, at pH=7.0 and at 30°C). A significant linear correlation between color yields and increasing nano-TiO_2 concentrations was observed (R^2=0.84, F=13.76, p=0.01) (Table 12, SET 4). 91.19%, 94.95% and 96.24% color yields were found in 0.5, 10 and 20 mg/L nano-TiO_2, respectively, after 150 min sonication time, at pH=7.0 and at 60°C (Table 12, SET 4). The contribution of nano-CeO_2 concentrations on color removals were 3.53%, 7.29% and 8.58% in 10, 100 and 1000 mg/L nano-CeO_2, respectively, after 150 min sonication time, at pH=7.0 and at 60°C, compared to the control (E=87.66% color after

T[a]	Phenols[b]	Polyphenols Removal Efficiencies[b]																	
		nano-CeO_2[c]						nano-TiO_2[c]						nano-CeO_2/TiO_2[c]					
		10[c]		100[c]		1000[c]		0.5[c]		10[c]		20[c]		100[c]		500[c]		1000[c]	
		120[d]	150[d]	120[d]	150[d]	120[d]	150[d]	120[d]	150[d]	120[d]	150[d]	120[d]	150[d]	120[d]	150[d]	120[d]	150[d]	120[d]	150[d]
25[a]	PHE R[b]	59	73	63	79	66	80	60	75	64	82	67	83	61	76	69	85	71	87
	4-MP R[b]	48	68	51	72	54	73	49	69	52	75	55	76	50	70	56	77	59	80
	4-H R[b]	44	66	46	69	49	70	45	67	47	72	50	73	46	68	50	73	55	76
	2-M-4-H R[b]	41	61	42	63	45	64	42	62	43	65	46	67	43	63	45	66	48	70
30[a]	PHE R[b]	64	83	67	87	70	88	65	84	69	89	72	91	66	85	74	90	76	92
	4-MP R[b]	54	79	56	82	59	84	55	80	58	87	61	87	56	81	62	88	66	90
	4-H R[b]	51	73	52	75	55	78	52	74	54	79	57	80	53	75	57	80	59	82
	2-M-4-H R[b]	48	67	50	68	51	71	49	68	50	71	53	73	50	69	52	72	55	76
60[a]	PHE R[b]	72	91	74	92	77	94	73	92	77	93	80	95	74	93	82	94	86	96
	4-MP R[b]	60	84	61	86	64	89	61	85	64	90	67	92	62	86	68	92	72	93
	4-H R[b]	55	78	57	80	59	83	56	79	58	84	61	85	57	80	61	86	67	88
	2-M-4-H R[b]	52	75	54	77	56	80	53	76	54	79	57	81	54	77	56	82	64	85

Table 14: Measurements of total phenols and three polyphenols (4-methyl phenol, 4-hydorxyanisole and 2-methyl-4-hyroxyanisole) in TI ww with the addition of different nano-CeO_2, nano-TiO_2 and nano-CeO_2/TiO_2 concentrations with GC-MS after 120 and 150 min sonication time, at pH=7, at increasing temperatures (25, 30 and 60°C), at initial total phenol concentration=37 mg/L, at sonication power=640 W and at sonication frequency=35 kHz (n=3, mean values).

PHE R: Total phenol removal efficiency (%), 4-MP R: 4-methyl phenol removal efficiency (%), 4-H R: 4-hydorxyanisole removal efficiency (%), 2-M-4-H R: 2-methyl-4-hyroxyanisole removal efficiency (%), a : (°C), b : removal efficiency (%), c : mg/L, d : min.

150 min sonication time, at pH=7.0 and at 60°C). The maximum color removal was 96.24% in nano-TiO_2=20 mg/L after 150 min sonication time, at pH=7.0 and at 60°C. A significant linear correlation between color yields and increasing nano-TiO_2 concentrations was observed (R2=0.87, F=16.73, p=0.01) (Table 12, SET 4). In the presence of TiO_2 active radicals produced. The reason would be due to increased surface area of TiO_2 powder which provides more active sites to produce radicals. However, the most ideal condition for dye degradation could be achieved by simultaneous usage of US and TiO_2 with H_2O_2 [58,131]. Methylene Blue and Rhodamine B dyestuffs were selected for our study. It is expected that the sonolytic degradation of Methylene Blue and Rhodamine B dyestuff would mainly occur by $OH^\bullet$ attack [96,97]. In order to investigate the dependence of the $OH^\bullet$ during the degradation of Methylene Blue and Rhodamine B dyestuffs by ultrasonic irradiation, the sonolytic degradation of Methylene Blue and Rhodamine B in the presence of radical scavengers (such as $H^\bullet$, $OH^\bullet$, $O_2H^\bullet$, $O_2^\bullet$), known as an effective $OH^\bullet$ scavenger, was performed and was to scavenge $OH^\bullet$ in the bubble and prevent the accumulation of $OH^\bullet$ at the interface of the bubble [96,97]. Wang et al. [57] obtained 60% color yield in a TI ww containing 100 mg/L Azo Funchsine solution at 40 kHz, at 50 W after 60 min sonication time, at 30°C with TiO_2=50 mg/L. In a study performed by Abbasi and Asl [58] 90% color removal achieved in a TI ww containing 15 mg/L Basic Blue 41, at 35 kHz, at 160 W, after 180 min sonication time at 30°C with TiO_2=100 mg/L. In this study, 90.13% color removal was found in nano-TiO_2=20 mg/L after 150 min sonication time and at 30°C. The color yield in the present study is higher than the yield obtained by Wang et al. [57] at 30°C and by Abbasi and Asl [58] at 30°C as mentioned above. This could be attributed to the differentiations in dyes present in TI to the operational conditions such as sonication time, sonication frequency, dyestuff properties and sonication power.

83% PHE R, 76% 4-MP, 73% 4-H and 67% 2-M-4-H polyphenols removals were observed in nano-TiO_2=20 mg/L after 150 min sonication time, respectively, at pH=7.0 and at 25°C (Table 14). 13% PHE R, 11% 4-MP, 9% 4-H and 7% 2-M-4-H increase in polyphenols removals were obtained in nano-TiO_2=20 mg/L after 150 min sonication time, respectively, at pH=7.0 and at 25°C, compared to the control (without nano-TiO_2 while E=70% PHE R, E=65% 4-MP, E=64% 4-H and E=60% 2-M-4-H polyphenols after 150 min sonication time, at pH=7.0 and at 25°C. A significant linear correlation between polyphenols yields and increasing nano-TiO_2 concentrations was observed (R^2=0.97, F=18.11, p=0.01) (Table 14). 91% PHE R, 87% 4-MP, 80% 4-H and 73% 2-M-4-H polyphenols removals were observed in nano-TiO_2=20 mg/L after 150 min sonication time, respectively, at pH=7.0 and at 30°C (Table 14). 13% PHE R, 12% 4-MP, 10% 4-H and 8% 2-M-4-H increase in polyphenols removals were obtained in nano-TiO_2=20 mg/L after 150 min sonication time, respectively, at pH=7.0 and at 30°C compared to the control (E=78% PHE R, E=75% 4-MP, E=70% 4-H and E=65% 2-M-4-H polyphenols after 150 min sonication time, at pH=7.0 and at 30°C). A significant linear correlation between polyphenols yields and increasing nano-TiO_2 concentrations was obtained (R^2=0.92, F=18.62, p=0.01) (Table 14). 95% PHE R, 92% 4-MP, 85% 4-H and 81% 2-M-4-H polyphenols yields were found in nano-TiO_2=20 mg/L after 150 min sonication time, respectively, at pH=7.0 and at 60°C (Table 14). 10% PHE R, 13% 4-MP, 11% 4-H and 9% 2-M-4-H increase in polyphenols removals were obtained in nano-TiO_2=20 mg/L after 150 min sonication time, respectively, at pH=7.0 and at 60°C, compared to the control (E=85%

PHE R, E=79% 4-MP, E=74% 4-H and E=72% 2-M-4-H polyphenols after 150 min sonication time, at pH=7.0 and at 60°C). The maximum polyphenols removals were 95% PHE R, 92% 4-MP, 85% 4-H and 81% 2-M-4-H in nano-TiO_2=20 mg/L after 150 min sonication time, respectively, at pH=7.0 and at 60°C. A significant linear correlation between polyphenols yields and increasing nano-TiO_2 concentrations was found (R^2=0.84, F=16.75, p=0.01) (Table 13). The increase in sono-destruction yields for phenol after 120 min sonication time, at high TiO_2 concentrations (>10 mg/L) may be explained by the fragmentation of TiO_2 catalyst which by the cavitation process produces higher surface area [132]. Throughout sonication ultrasonic waves not only destroy the phenol compounds through cavitation process but also could increases the adsorption process by increasing the surface area of the TiO_2 catalyst as reported by Laxmi et al. [132]. During the US of TI ww with TiO_2, the H_2O_2 form more active free radicals, such as $OH^{\bullet}$ and $O_2H^{\bullet}/O_2^{-1}$ [132].

The attack of $OH^{\bullet}$ on phenol was confined through sonication. The formation of the hydrophenols through sonication can be explained by the Equatins (17), (18) and (19):

$$H_2O \rightarrow H^{\bullet} + OH^{\bullet} \quad (17)$$

$$OH^{\bullet} + OH^{\bullet} \rightarrow H_2O_2 \quad (18)$$

$$Phenol + OH^{\bullet} \rightarrow Dihydroxyphenols \quad (19)$$

Effect of nano-cerium dioxide/titanium dioxide (nano-CeO_2/TiO_2) concentrations on the removal of COD_{dis}, color and polyphenols versus increasing sonication time and temperature

Nano-CeO_2/TiO_2 = 100, 500 and 2000 mg/L (the ratios of 1/4, 1/1, 4/1, 9/1, w/w) and nano-CeO_2/TiO_2 ratio concentrations were applied to nano-CeO_2=20 mg/L / nano-TiO_2=80 mg/L, nano-CeO_2=50 mg/L / nano-TiO_2=50 mg/L, nano-CeO_2=80 mg/L / nano-TiO_2=20 mg/L, nano-CeO_2=90 mg/L / nano-TiO_2=10 mg/L, nano-CeO_2=100 mg/L / nano-TiO_2=400 mg/L, nano-CeO_2=250 mg/L / nano-TiO_2=250 mg/L, nano-CeO_2=400 mg/L/ nano-TiO_2=100 mg/L, nano-CeO_2=450 mg/L / nano-TiO_2=50 mg/L, nano-CeO_2=400 mg/L / nano-TiO_2=1600 mg/L, nano-CeO_2=1000 mg/L / nano-TiO_2=1000 mg/L, nano-CeO_2=1600 mg/L / nano-TiO_2=400 mg/L, nano-CeO_2=1800 mg/L / nano-TiO_2=200 mg/L, respectively. 88.41%, 92.15% and 97.39% COD_{dis} removals were observed in 100, 500 and 1000 mg/L nano-CeO_2/TiO_2, respectively, after 150 min sonication time, at pH=7.0 and at 30°C (Table 11, SET 5). 6.88%, 10.62% and 15.86% increase in COD_{dis} removals were obtained in 100, 500 and 1000 mg/L nano-CeO_2/TiO_2, respectively, after 150 min sonication time, at pH=7.0 and at 30°C, compared to the control (without nano-CeO_2/TiO_2 while E=81.53% COD_{dis} after 150 min sonication time, at pH=7.0 and at 30°C). A significant linear correlation between COD_{dis} yields and increasing nano-CeO_2/TiO_2 concentrations was observed (R^2=0.79, F=10.14, P=0.01) (Table 11, SET 2 and SET 5). 91.18%, 97.20% and 99.37% COD_{dis} yields were obtained in 100, 500 and 1000 mg/L nano-CeO_2/TiO_2, respectively, after 150 min sonication time, at pH=7.0 and at 60°C (Table 11, SET 5). The contribution of nano-CeO_2/TiO_2 concentrations on COD_{dis} removals were 6.26%, 12.28% and 14.45% in 100, 500 and 1000 mg/L nano-CeO_2/TiO_2, respectively, after 150 min sonication time, at pH=7.0 and at 60°C, compared to the control (E=84.92% after 150 min sonication time, at pH=7.0 and at 60oC) (Table 11, SET 2 and SET 5). The maximum COD_{dis} removal was 99.37% in a 1000 mg/L concentrations of nano-CeO_2/TiO_2 after 150 min sonication time, at pH=7.0 and at 60°C. A significant linear correlation between COD_{dis} yields and increasing nano-CeO_2/TiO_2 concentrations was observed (R^2=0.78, F=12.83, P=0.01) (Table 11, SET 5).

The mechanisms of COD_{dis} removal were determined the average crystal size of CeO_2 decreased and the surface areas increased; the low valence of Ce^{3+} increase, and the chemisorbed O_2 slightly decreased with the increase of Ti content on the surface of CeO_2-TiO_2 catalysts. TiO_2 is a promising material both as an active material and a support for some catalytic reaction [133,134]. On the other hand, the fact that Ti^{+4} has the lower ionic radius than Ce^{+4} indicates that Ce^{+4} in the CeO_2 lattice could be replaced by Ti^{+4}, so that a fluorite structure solid solution could be formed, and improve the properties of pure CeO_2 [133,134]. Nano-CeO_2/TiO_2 mixed oxides at ratios of 1/1, 1/4 showed higher activity than the pure nano-CeO_2 and pure nano-TiO_2. Yang et al. [135] investigated the cataliytic activity of CeO_2/TiO_2 catalysts of 1000 mg/L phenol in batch and packed-bed reactors. CeO_2/TiO_2 mixed oxides show the higher activity than pure CeO_2, pure TiO_2 and CeO_2/TiO_2=1/1 displays the highest phenol removal. In the batch reactor, 100% COD yield is measured after 120 min sonication time. In a packed-bed reactor using a CeO_2 to TiO_2 ratio of 1/1, over 91% COD removal is obtained at an initial COD concentration of 1000 mg/L for 100 h continuous reaction. Leaching of metal ions at the aforementioned CeO_2 to TiO_2 ratio is very low during the continuous reaction [135]. Zhao et al. [98] showed that the Fe/TiO_2-CeO_2 was a very efficient catalyst to oxidize the pollutants of dye industry such as H-acid (1-amino-8-hydroxynaphthalene-3,6-disulfonic acid that an important dye intermediate, is produced from naphthalene by a combination of the unit processes of sulfonation, nitration, reduction, and hydrolysis, and it is used in the manufacture of a large number of azo dyes and pigments) into biodegradable species and doping Ce into TiO_2. This greatly enhancing the surface areas of the catalysts. 89.60% and 70% COD yields were obtained at Fe/TiO_2-CeO_2=1000 g and at a Ti to Ce ratio of 1/1 at 100°C, at pH=5.0 after 90 min sonication time. Gao et al. [136] investigated high surface area and good redox ability are important to the catalytic activity, while the strong interaction between CeO_2 and TiO_2 as well as high concentration of amorphous or highly dispersed nano-crystalline CeO_2 should be the reason for the excellent performance of the catalyst. 70-98% Nitric Oxide (NO) convertion was measured with CeO_2/TiO_2=1/2 and CeO_2=1000 mg/L/TiO_2=2000 mg/L, at [O_2], N_2 (g) levels of 3% and 500 mL/min in the presence of 500-1000 mg/L [NO] = [NH_3] (Ammonia) concentrations at 300°C. 35-98% NO convertion with 200 mg/L Sulfur dioxide (SO_2) was observed with CeO_2/TiO_2, and [NO] = [NH_3] =1000 mg/L at 150 min sonication time and at 350°C. In this study, 99.37% COD_{dis} removal was found in nano-CeO_2/TiO_2=1000 mg/L after 150 min sonication time and at 60°C. The COD_{dis} yield in the present study is higher than the yield obtained by Yang et al. [135], by Zhao et al. [98] and by Gao et al. [136]. This could be atributed that differences between treatment methods, catalysts properties, sonication temperature and sonication time in TI ww. Deng et al. [137] found higher sorption capacity for 9.40 mg/g Arsenic (As^{+5}) at pH=6.5 with mixed of nano-CeO_2/TiO_2 adsorbent than both the pure nano-TiO_2 and pure nano-CeO_2 adsorbents. The amorphous composition of Ce-Ti hybrid adsorbent, and the nano sized levels were related to the high sorption capacity for as+5.

89.31%, 91.07% and 93.42% color yields were observed in 100,

500 and 1000 mg/L nano-CeO_2/TiO_2, respectively, after 150 min sonication time, at pH=7.0 and at 30°C (Table 12, SET 5). 11.05%, 12.81% and 15.16% increase in the color removals were obtained in 100, 500 and 1000 mg/L nano-CeO_2/TiO_2, respectively, after 150 min sonication time, at pH=7.0 and at 30oC, compared to the control (E=78.26% color after 150 min sonication time, at pH=7.0 and at 30°C). A significant linear correlation between color yields and increasing nano-CeO_2/TiO_2 concentrations was not observed (R^2=0.33, F=0.25, P=0.01) (Table 12, SET 2 and SET 5). 91.42%, 95.89% and 98.07% color yields were found in 100, 500 and 1000 mg/L nano-CeO_2/TiO_2, respectively, after 150 min sonication time, at pH=7.0 and at 60°C (Table 12, SET 5). The contribution of nano-CeO_2/TiO_2 concentrations on color removals were 3.76%, 8.23% and 10.41% in 100, 500 and 1000 mg/L nano-CeO_2/TiO_2, respectively, after 150 min sonication time, at pH=7.0 and at 60°C, compared to the control (E=87.66% color after 150 min sonication time, at pH=7.0 and at 60°C) (Table 12, SET 2 and SET 5). The maximum color removal was 98.07% in nano-CeO_2/TiO_2=1000 mg/L after 150 min sonication time, at pH=7.0 and at 60°C. A significant linear correlation between color yields and increasing nano-CeO_2/TiO_2 concentrations was not obtained (R^2=0.30, F=0.17, P=0.01) (Table 12, SET 5).

The average crystal size of CeO_2 decreased and the surface areas increased during sonication; the low valence of Ce^{+3} increased, and the chemisorbed O_2 slightly decreased with the increase of Ti content on the surface of CeO_2-TiO_2 catalysts as reported by Yang et al. [138]. Decolorization ratio increased during sonication with high CeO_2-TiO_2 concentrations (2000, 5000, 7500 mg/L). Nano-CeO_2/TiO_2 was a very efficient catalyst to oxidize the pollutants of dye industry into biodegradable species and doping Ce into TiO_2 obviously restrained the growth of crystal, greatly enhancing the surface areas of the catalysts. However, the large surface area of nano-CeO_2/TiO_2 catalyst was increased to degradation efficiencies and degradation rate during sonication period. The activity of nano-TiO_2/CeO_2 catalysts was strongly affected by Ti/Ce molar ratio. High Ti/Ce ratio was expanded to degradation rate of nano-TiO_2/CeO_2 catalysts, degradation efficiencies of pollution compounds (COD, color, polyphenols, TAAs, etc.) [138]. Shirsath et al. [139] exhibited the synthesis of TiO_2 NPs doped with Fe and Ce catalysts prepared by sonochemical method higher photocatalytic activity as compared to the catalysts prepared by the conventional doping methods. 85% Crystal Violet removal in 0.80 mol% Ce-TiO_2, 80% Crystal Violet removal in 1.20 mol% Fe-TiO_2, 75% Crystal Violet removal in 1 mol% TiO_2, respectively, after 100 min sonication time and at pH=6.5. Wang et al. [140] investigated that the CeO_2/TiO_2, SnO_2/TiO_2 and ZrO_2/TiO_2 composites were prepared by dispersing various nano-sized oxides (CeO_2, SnO_2, ZrO_2, TiO_2) with US and mixing TiO_2/CeO_2, SnO_2/ZrO_2, respectively, in boiling H_2O in a molar ratio of 4/1, followed by calcining at 500°C for 60 min. The sonocatalytic degradation of Acid Red B was measured to 91.32% in CeO_2/TiO_2, 67.41% in SnO_2/TiO_2, 65.26% in TiO_2, 41.67% in ZrO_2/TiO_2, 28.34% in SnO_2, 26.75% in CeO_2, 23.33% in ZrO_2, 16.67% in only US, respectively, at pH=5, at 50°C and at 60 min sonication time. Methyl Violet removal was observed to 40% in TiO_2, 25% in ZrO_2/TiO_2, 55% in SnO_2/TiO_2, 50% in CeO_2/TiO_2, respectively, at pH=5, at 50°C and at 60 min sonication time. Rhodamine B yield was found to 30% in TiO_2, 9% in ZrO_2/TiO_2, 32% in SnO_2/TiO_2, 38% in CeO_2/TiO_2, respectively, at pH=5, at 50°C and at 60 min sonication time. In this study, 98.07% color removal was measured in nano-CeO_2/TiO_2=1000 mg/L after 150 min sonication time and at 60°C. The color yield in the present study is higher than the yield observed by Shirsath et al. [139], by Wang et al. [140] at 50°C as mentioned above. This could be atributed that differences between dyestuff properties, sonication time and sonication temperature in TI ww. Zhao et al. [98] investigated that Fe/TiO_2-CeO_2 (Ti/Ce 9/1, 2 wt.% Fe) was a very efficient catalyst to oxidize the pollutants of dye industry such as H-acid into biodegradable species and doping Ce into TiO_2 obviously restrained the growth of crystal, greatly enhancing the surface areas of the catalysts. 98.1% and 90% color removals were observed at Fe/TiO_2-CeO_2=1 g and at Ti/Ce=9/1, at 100°C, at initial pH=5.0, at 90 min sonication time, at 1 atm and at H_2O_2=17.6 mL, respectively. In this study, 98.07% color removal was obtained in nano-CeO_2/TiO_2=1000 mg/L after 150 min sonication time and at 60°C. The color yield in the present study is similar result observed by Zhao et al. [98] at 100°C as mentioned above 87% PHE R, 80% 4-MP, 76% 4-H and 70% 2-M-4-H polyphenols removals were observed in nano-CeO_2/TiO_2=1000 mg/L after 150 min sonication time, respectively, at pH=7.0 and at 25°C (Table 14). 17% PHE R, 15% 4-MP, 12% 4-H and 10% 2-M-4-H increase in polyphenols removals were obtained in nano-CeO_2/TiO_2=1000 mg/L after 150 min sonication time, respectively, at pH=7.0 and at 25°C, compared to the control (E=70% PHE R, E=65% 4-MP, E=64% 4-H, E=60% 2-M-4-H polyphenols after 150 min sonication time, at pH=7.0 and at 25°C). A significant linear correlation between polyphenols yields and increasing nano-CeO_2/TiO_2 concentrations was observed (R^2=0.84, F=11.25, P=0.01) (Table 13 and Table 14). 92% PHE R, 90% 4-MP, 82% 4-H and 76% 2-M-4-H polyphenols removals were observed in nano-CeO_2/TiO_2=1000 mg/L after 150 min sonication time, respectively, at pH=7.0 and at 30°C (Table 14). 14% PHE R, 15% 4-MP, 12% 4-H and 11% 2-M-4-H increase in polyphenols removals were obtained in nano-CeO_2/TiO_2=1000 mg/L after 150 min sonication time, respectively, at pH=7.0 and at 30°C, compared to the control (E=78% PHE R, E=75% 4-MP, E=70% 4-H, E=65% 2-M-4-H polyphenols after 150 min sonication time, at pH=7.0 and at 30°C). A significant linear correlation between polyphenols removals and increasing nano-CeO_2/TiO_2 concentrations was found (R^2=0.73, F=12.38, P=0.01) (Table 13 and Table 14). 96% PHE R, 93% 4-MP, 88% 4-H and 85% 2-M-4-H polyphenols yields were found in nano-CeO_2/TiO_2=1000 mg/L after 150 min sonication time, respectively, at pH=7.0 and at 60oC (Table 14). 11% PHE R, 14% 4-MP, 14% 4-H and 13% 2-M-4-H polyphenols increase in polyphenols removals were obtained in nano-CeO_2/TiO_2=1000 mg/L after 150 min sonication time, respectively, at pH=7.0 and at 60°C, compared to the control (E=85% PHE R, E=79% 4-MP, E=74% 4-H, E=72% 2-M-4-H polyphenols after 150 min sonication time, at pH=7.0 and at 60°C). The maximum polyphenols removals were 96% PHE R, 93% 4-MP, 88% 4-H and 85% 2-M-4-H in nano-CeO_2/TiO_2=1000 mg/L after 150 min sonication time, respectively, at pH=7.0 and at 60°C. A significant linear correlation between polyphenols removals and increasing nano-CeO_2/TiO_2 concentrations was obtained (R^2=0.86, F=14.37, P=0.01) (Table 13 and Table 14). 99.37% COD_{dis}, 98.07% color, 96% total phenol (PHE R), 93% 4-MP, 88% 4-H and 85% 2-M-4-H maximum removal efficiencies were found in the reactor containing nano-CeO_2/TiO_2=1000 mg/L ([nano-CeO_2=500 mg/L / nano-TiO_2=500 mg/L]=1/1) after 150 min sonication time and at 60°C (Tables 11-14).

The obtained nano-CeO_2/TiO_2 materials exhibit large specific surface area and uniform pore sizes [141]. Introduction of nano-CeO_2 species can effectively extend the spectral response from visible area and enhance the surface hydroxyl groups of the mesoporous TiO_2. The CeO_2/TiO_2 nanocomposites show high photocatalytic activity in the degradation of the p-chlorophenol aqueous solution under the vis-

ible irradiation [141]. The CeO_2/TiO_2, SnO_2/TiO_2 and ZrO_2/TiO_2 composites were prepared by dispersing various nano-sized oxides (CeO_2, SnO_2, ZrO_2 and TiO_2) with US and mixing TiO_2 with CeO_2, SnO_2 and ZrO_2, respectively, in boiling H_2O in a molar ratio of 4/1, followed by calcining temperature 500°C for 60 min [140]. Titanium isopropanoids and propanol were added in US reactor for 5 min sonication time [139]. After, sodium hydroxide (NaOH) and $[Ce(NO_3)_2{\cdot}6H_2O]$ were added in ultrasound reactor for 30 min sonication time. Then, compounds in US reactor were precipited and were dried after 30 min sonication time. After then, calcination process was applied to these compounds at US reactor at 450°C for 180 min. Finally, synthesis of Ce doped with TiO_2 were occured by sonochemical method [139].

To study the effect of preparation method on the photocatalytic activity of the catalysts prepared by sonochemical and the conventional method, the experiments were conducted for 2% (mol %) of Ce and Fe doped TiO_2 and pure TiO_2. It is observed that the degradation of crystal violet increased gradually with UV irradiation time for all the samples. The highest degradation (84%) was achieved with Ce–TiO_2 (US) sample followed by Fe–TiO_2 (US) (77%) and undoped TiO_2 (US) sample gave 71% degradation. The samples prepared by conventional method resulted in 75, 68 and 61% degradation for Ce–TiO_2 (CV), Fe–TiO_2 (CV) and TiO_2 (CV) respectively. Maximum extent of degradation for the Cerium doping can be attributed to the fact that cerium shows the enhanced photo-response in the visible region and the redox pair of cerium (Ce^{+3}/Ce^{+4}) is also important, since cerium could act as an effective electron scavenger to trap the bulk electrons in TiO_2 [16]. The preparation method played an important role in deciding the photoactivity of a catalyst. It was observed that the catalysts prepared by sonochemical method showed higher activity against catalyst prepared by the conventional method, possibly attributed to the higher surface area for the reaction due to the lower particle size of the catalyst achieved with the sonochemical method. The increased high-velocity interparticle collisions among the particles can result in the fragmentation of the TiO_2 particles leading to lower size in the case of sonochemical method. Also ultrasonic irradiation may accelerate the hydrolysis and formation of titania crystals. Further sonication method can evenly disperse the metal ions into the crystal lattice of TiO_2, independent of whether the ions react with Ti–gel or not [36]. This study clearly demonstrates the importance and advantages of sonication in the modification and improvement of the photocatalytic properties of TiO_2 and doped TiO_2 catalysts. After the first set of experiments, as it was observed that all the samples prepared by sonochemical method gives higher degradation than the samples prepared by conventional method, the studies related to the effect of other operating parameters on the degradation process were performed with the catalyst prepared by sonochemical method [139].

The CeO_2/TiO_2 heterostructure with stable structure canbe constructed by directly combining the crystal structure of cerium dioxide and titanium dioxide. However, due to the largedifference of the radius between the titanium atom and thecerium atom, lattice distortion will be caused when cerium atom is substituted [142], resulting in lattice structure mis-match, high crystal energy, and difficulties in stabilization [142]. For TiO_2, the minimum conduction band is located at G point, andthe maximum valence band is located at Z point, indicating anindirect band gap. The calculated band gap is 3.061 eV, whichis smaller than the experimental value of 3.2 eV [142]. The density of states of TiO_2, where the range of -5 eV to 0 eV below the Fermi level is the valence band region, which ismainly contributed by the O_2p orbit, and the range of 2.5-15 eV above the Fermi level is the conduction band region, which is mainly contributed by the Ti3d orbit. The results showed that theband gap of the CeO_2/TiO_2 heterostructure is significantlysmaller than that of TiO_2 (3.061 eV), which reduces the energyneeded to excite photons and improves the optical absorption capacity. The heterostructure changes the response range of light, widens the original UV region to the visible region, greatly improves the utilization of visible light, and is expectedto be widely used in the field of photocatalysis [142].

Compared with the powder photocatalysts, the substrate photocatalysts are more practical in water disinfection because of their specific properties such as easy in recovery and high reusability [143]. However, the low sterilization efficiency of substrate photocatalysts limit its further applications. Here, we prepared a binary composite direct Z-scheme heterojunction CeO_2/TiO_2 nanotube arrays (CeO_2/TiO_2 NTAs) to improve the photocatalytic disinfection performance [143]. The heterojunction realized the spatial separation between the oxidation site and the reduction site under light irradiation. Consequently, it was favorable to produce ROS ($^{\bullet}O_2^-$, OH,$^{\bullet}O_2$) and showed a good antibacterial effect on both Gram-positive and negative bacteria (98.8 %). In addition, the results of the cyclic sterilization experiment showed that the sterilization efficiency of the CeO_2/TiO_2 NTAs still reached 98.3 % after 3 times of recycling and reuse. Furthermore, the material still maintains a good sterilization effect and recovery performance in practical applications [143].

Conclusion

Low frequency (35 kHz) sonication proved to be a viable tool for the effective of COD_{dis}, color, polyphenols removals in TI ww. The contribution of increasing nano-TiO_2, nano-CeO_2 and nano-CeO_2/TiO_2 addition concentrations were significant to the removals of COD_{dis}, color and polyphenols in increasing sonication time compared to the control at pH=7.0 and at 25°C.

96.70% COD_{dis}, 95.06% color, 94% PHE R, 89% 4-MP, 83% 4-H and 80% 2-M-4-H maximum removals were observed in the reactor containing nano-CeO2=1000 mg/L after 150 min sonication time, at Ti/Ce=1/1 and at 60°C. 98.13% COD_{dis}, 96.24% color, 95% PHE R, 92% 4-MP, 85% 4-H and 81% 2-M-4-H maximum yields were obtained in the reactor containing nano-TiO_2=20 mg/L after 150 min sonication time, at Ti/Ce=1/1 and at 60°C. 99.37% COD_{dis}, 98.07% color, 96% PHE R, 93% 4-MP, 88% 4-H and 85% 2-M-4-H maximum removals were obtained in the reactor containing nano-CeO_2/TiO_2=1000 mg/L after 150 min sonication time, at Ti/Ce=1/1 and at 60°C. Eachone of increasing nano-TiO_2 and nano-CeO_2 concentrations were increased to the COD_{dis}, color and polyphenols removals in TI ww at sonication experiments. Also, increasing temperature was positively effected in TI ww at sonication time. Although, the nano-CeO_2/TiO_2 materials to exhibit large specific surface area and uniform pore sizes. Introduction of nano-CeO_2 species can effectively extend the spectral response from visible area and enhance the surface hydroxyl groups of the mesoporous nano-TiO_2. In addition to, large surface area and uniform NPs pore sizes of nano-CeO_2/TiO_2 to increase the degradation rates of pollutions (COD_{dis}, color and polyphenols) and the degradation efficiencies of pollutions (COD_{dis}, color and polyphenols) in TI ww. The addition of nano-CeO_2/TiO_2 in TI ww was increased to removal efficiencies of pollutions (COD_{dis}, color and polyphenols) higher than the eachone of nano-CeO_2 and nano-TiO_2

catalysts additions in TI ww.

The sonication process could prove to be less land-intensive, less expensive and require less maintenance than traditional biological treatment processes and other advanced oxidation processes (AOPs). Sonication technology can provide a cost-effective alternative for destroying and detoxifying refractory compounds in TI ww.

Acknowledgement

This research study was undertaken in the Environmental Microbiology Laboratury at Dokuz Eylül University Engineering Faculty Environmental Engineering Department, Izmir, Turkey. The authors would like to thank this body for providing financial support.

References

1. Hielscher T (2005) Ultrasonic production of nano-size dispersions and emulsions, Dr. Hielscher GmbH, Warthestrasse 21, 14513 Teltow, Germany, ENS'05 Paris, France.
2. Yavuz CT, Mayo JT, Yu WW, Prakash A, Falkner JC (2006) Low-field magnetic separation of monodisperse Fe_3O_4 nanocrystals. Science 314: 964-967.
3. Recillas S, Colón J, Casals E, González E, Puntes V (2010) Chromium VI adsorption on cerium oxide nanoparticles and morphology changes during the process. Journal of Hazardous Materials 184: 425-431.
4. Özen AS, Aviyente V, Tezcanli-Güyer G, Ince NH (2005) Experimental and modeling approach to decolorization of azo dyes by ultrasound: Degradation of the hydrazone tautomer. The Journal of Physical Chemistry A 109: 3506-3516.
5. Tezcanli-Guyer G, Ince NH (2003) Degradation and toxicity reduction of textile dyestuff by ultrasound, Ultrasonics Sonochemistry 10: 235-240.
6. Crum LA (1995) Comments on the evolving filed of sonochemistry by a cavitation physicist. Ultrasonics Sonochemistry 2: 147-152.
7. Mason TJ, Pétrier C (2004) Advanced oxidation processes for water and wastewater treatment, in: Parson S. (editor). Ultrasound processes, IWA Publishing, London, 185-208.
8. Trovarelli A, de Leitenburg C, Boaro M, Dolcetti G (1999) The utilization of ceria in industrial catalysis. Catalysis Today 50: 353-367.
9. Luo MF, Yan ZL, Jin LY, He M (2006) Raman spectroscpopic study on the structure in the surface and the bulk shell of CexPr1-Xo2-δ mixed oxides. The Journal of Physical Chemistry B 110: 13068-13071.
10. Pradhan GK, Parida KM (2010) Fabrication of iron-cerium mixed oxide: An efficient photocatalyst for dye degradation. International Journal of Engineering Science and Technology 2: 53-65.
11. Asilturk M, Sayılkan F, Arpac E (2009) Effect of Fe^{3+} ion doping to TiO_2 on the photocatalytic degradation of Malachite Green dye under UV and visirradiation. J Photochem Photobiol A: Chem 203: 64-71.
12. Zhou M, Yu J, Cheng B (2006) Effects of Fe-doping on the photocatalytic activity of mesoporous TiO_2 powders prepared by an ultrasonic method. J Hazard Mater B 137: 1838-1847.
13. Nahar MS, Hasegawa K, Kagaya S, Kuroda S (2007) Comparative assessment of the efficiency of Fe-doped TiO_2 prepared by two doping methods and photocatalytic degradation of phenol in domestic water suspensions. Sci Technol Adv Mater 8: 286-291.
14. Abazovic ND, Mirenghi L, Jankovic IA, Bibic N, Sojic DV (2009) Synthesis and characterization of rutile TiO_2 nanopowders doped with iron ions, Nanoscale Res Lett 4: 518-525.
15. Luu CL, Nguyen QT, Ho ST (2010) Synthesis and characterization of Fe-doped TiO2 photocatalyst by the sol–gel method. Adv Nat Sci Nanosci: Nanotechnol 1: 1-5.
16. Silva AMT, Silva CG, Draz_ic´ G, Faria JL (2009) Ce-doped TiO_2 for photocatalytic degradation of chlorophenol. Catal Today 144: 13-18.
17. Shi ZL, Du C, Yao SH (2011) Preparation and photocatalytic activity of cerium doped anatase titanium dioxide coated magnetite composite. J Taiwan Inst Chem Eng 42: 652-657.
18. Wang J, Lv Y, Zhang L, Liu B, Jiang R (2010) Sonocatalytic degradation of organic dyes and comparison of catalytic activities of CeO_2/TiO_2, SnO_2/TiO_2 and ZrO_2/TiO_2 composites under ultrasonic irradiation. Ultrason Sonochem 17: 642-648.
19. Shon HK, Cho DL, Na SH, Kim JB, Park HJ (2009) Development of a novel method to prepare Fe- and Al-doped TiO_2 from wastewater. J Ind Eng Chem 15: 476-482.
20. Chang S, Liu W (2011) Surface doping is more beneficial than bulk doping to the photocatalytic activity of vanadium-doped TiO_2. App Catal B: Environ 101: 333-342.
21. Venkatachalam N, Palanichamy M, Arabindoo B, Murugesan V (2007) Enhanced photocatalytic degradation of 4-chlorophenol by Zr^{4+} doped nano TiO_2. J Mol Catal A: Chem 266: 158-165.
22. Zaleska A (2008) Doped- TiO2: A review. Recent Patents on Engineering 2: 157-164.
23. Rauf MA, Meetani MA, Hisaindee S (2011) an overview on the photocatalytic degradation of azo dyes in the presence of TiO_2 doped with selective transition metals. Desalination 276: 13-27.
24. Ghorai TK, Biswas SK, Pramanik P (2008) Photooxidation of different organic dyes (RB, MO, TB, and BG) using Fe (III)-doped TiO_2 nanophotocatalyst prepared by novel chemical method. Appl Surf Sci 254: 7498-7504.
25. Wang H, Niu J, Long X, He Y (2008) Sonophotocatalytic degradation of methyl orange by nano-sized Ag/ TiO_2 particles in aqueous solutions. Ultrason Sonochem 15: 386-392.
26. Anandan S, Ashokkumar M (2009) Sonochemical synthesis of Au–TiO_2 nanoparticles for the sonophotocatalytic degradation of organic pollutants in aqueous environment. Ultrason Sonochem 16: 316-320.
27. Koci K, Mateju K, Obalova L, Krejcikova S, Lacny´ Z (2010) Effect of silver doping on the TiO_2 for photocatalytic reduction of CO_2. App Catal B: Environ 96: 239-244.
28. Zhang QH, Han WD, Hong YJ, Yu JG (2009) Photocatalytic reduction of CO_2 with H_2O on Pt-loaded TiO_2 catalyst. Catal Today 148: 335-340.
29. Li X, Xiong R, Wei G (2009) Preparation and photocatalytic activity of nanoglued Sndoped TiO_2. J Hazard Mater 164: 587-591.
30. Kiriakidou FI, Kondarides DI, Verykios XE (1999) The effect of operational parameters and TiO_2-doping on the photocatalytic degradation of azo-dyes. Catal Today 54: 119-130.
31. Liu S, Chen X (2008) A visible light response TiO_2 photocatalyst realized by cationic S-doping and its application for phenol degradation. J Hazard Mater 152: 48-55.
32. Narayanan BN, Yaakob Z, Koodathil R, Chandralayam S, Sugunan S (2009) Malayattil, Photodegradation of methylorange over zirconia doped TiO_2 using solar energy. Eur J Sci Res 28: 566-571.
33. Yu JC, Yu J, Ho W, L. Zhang L (2001) Preparation of highly photocatalytic active nanosized TiO_2 particles via ultrasonic irradiation. Chem Commun 19: 1942-1943.
34. Neppolian B, Wang Q, Jung H, Choi H (2008) Ultrasonic-assisted sol-gel method of preparation of TiO_2 nano-particles: characterization, properties and 4-chlorophenol removal application. Ultrason Sonochem 15: 649-658.
35. Li H, Liu G, Chen S, Liu Q (2010) Novel Fe doped mesoporousTiO_2 microspheres: Ultrasonic–hydrothermal synthesis, characterization, and

photocatalytic properties. Physica E 42: 1844-1849.

36. Huang W, Tang X, Wang Y, Koltypin Y, Gedanken A (2000) Selective synthesis of anatase and rutile via ultrasound irradiation. Chem Commun 15: 1415-1416.

37. Wang XK, Wang C, Guo WL (2012) Sonochemical synthesis of nitrogen doped TiO_2 at a low temperature. Adv Mater Res 356: 403-406.

38. Yu J, Zhou M, Cheng B, Yu H, Zhao X (2005) Ultrasonic preparation of mesoporous titanium dioxide nanocrystalline photocatalysts and evaluation of photocatalytic activity. J Mol Catal A: Chem 227: 75-80.

39. Chen X, Mao SS (2007) Titanium dioxide nanomaterials: Synthesis, properties, modifications, and applications. Chem Rev 107: 2891-2959.

40. Zhu Y, Li H, Koltypin Y, Hacohen YR, Gedanken A (2001) Sonochemical synthesis of titania whiskers and nanotubes. Chem Commun 24: 2616-2617.

41. Huang W, Tang X, Felner I, Koltypin Y, Gedanken A (2002) Preparation and characterization of FexOy-TiO_2 via sonochemical synthesis. Mater Res Bull 37: 1721-1735.

42. Kusmierek E (2020) A CeO2 Semiconductor as a Photocatalytic and Photoelectrocatalytic Material for the Remediation of Pollutants in IndustrialWastewater: A Review Catalysts 10: 1435-1454.

43. Liu Y, Sun DZ (2007) Development of Fe_2O_3-CeO_2-TiO_2/gamma-Al_2O_3 as catalyst for catalytic wet air oxidation of methyl orange azo dye under room condition. Applied Catalysis B: Environmental 72: 205-211.

44. Chen D, Ray AK (1998) Photodegradation kinetics of 4-nitrophenol in TiO_2 suspensions. Water Research 32: 3223-3234.

45. Khodja AA, Sehili T, Pilichowski JF, Boule P (2001) Photocatalytic degradation of 2-phenylphenol on TiO_2 and ZnO in aqueous suspensions. Journal of Photochemical and Photobiology A: Chemistry 141: 231-239.

46. Fujishima A (1999) TiO_2 photocatalysis: Fundamentals and applications. BKC publisher.

47. Takabayashi S, Nakamura R, Nakato Y (2004) A nano-modified Si/TiO_2 composite electrode for efficient solar water splitting. Journal of Photochemistry and Photobiology A: Chemistry 166: 107-113.

48. Bjorklund GC, Baer TM (2007) Organic thin film solar cell research conducted at Stanford University. Photonics Spectra 41: 70-76.

49. Entezari MH, Petrier C (2005) A combination of ultrasound and oxidative enzyme: Sono-enzyme degradation of phenols in a mixture. Ultrasonics Sonochemistry 12: 283-288.

50. Khokhawala IM, Gogate PR (2010) Degradation of phenol using a combination of ultrasonic and UV irradiations at pilot scale operation. Ultrasonics Sonochemistry 17: 833-838.

51. Wu C, Liu X, Wei D, Fan J, Wang L (2001a) Photosonochemical degradation of phenol in water. Water Research 35: 3927-3933.

52. Wu C, Wei D, Fan J, Wang L (2001b) Photosonochemical degradation of trichloroacetic acid in aqueous solution. Chemosphere 44: 1293-1297.

53. Kidak R, Ince NH (2007) Catalysis of advanced oxidation reactions by ultrasound: A case study with phenol. Journal of Hazardous Materials 146: 630-635.

54. Shirgaonkar IZ, Pandit AB (1998) Sonophotochemical destruction of aqueous solution of 2,4,6-trichlorophenol. Ultrasonics Sonochemistry 5: 53-61.

55. Cardoso SM, Mafra I, Reis A, Nunes C, Saraiva JA (2010) Naturally fermented black olives: Effect on cell wall polysaccharides and on enzyme activities of Taggiasca and Conservolea varieties. LWT-Food Science and Technology 43: 153-160.

56. Mrowetz M, Pirola C, Selli E (2003) Degradation of organic water pollutants through sonophotocatalysis in the presence of TiO_2. Ultrasonics Sonochemistry 10: 247-254.

57. Wang J, Sun W, Zhang Z, Jiang Z, Wang X (2008) Preparation of Fe-doped mixed crystal TiO_2 catalyst and investigation of its sonocatalytic activity during degradation of azo funchsine under ultrasonic irradiation. Journal of Colloidal and Interface Science 320: 202-209.

58. Abbasi M, Asl NR (2008) Sonochemical degradation of Basic Blue 41 dye assisted by nano TiO_2 and H_2O_2. Journal of Hazardous Materials 153: 942-947.

59. Wu C-H, Yu C-H (2009) Effects of TiO_2 dosage, pH and temperature on decolorization of C.I. Reactive Red 2 in a UV/US/TiO_2 system. Journal of Hazardous Materials 169: 1179-1183.

60. Baird RB, Eaton AD, Rice EW (editors). Standard Methods for the Examination of Water and Wastewater. (23th edn). Washington, DC: American Public Health Association (APHA), American Water Works Association (AWWA), Water Environment Federation (WEF). AWWA catalog no: 10086, ISBN: 9780875532875, American Public Health Association 800 I Street, NW, 20001-3770, Washington DC, USA. 2017.

61. Olthof M, Eckenfelder WWJr (1976) Coagulation of textile wastewater. Textile, Chemistry and Colorists 8: 18-22.

62. Eckenfelder WWJr (1989) Industrial Water Pollution Control (2nd ed). Signapore: McGraw-Hill Inc.

63. Tok AIY, Boey FYC, Dong Z, Sun XL (2007) Hydrothermal synthesis of CeO_2 nanoparticles. Journal of Materials Processing Technology 190: 217-222.

64. Zar JH (1984) Biostatistical Analysis. Prentice-Hall, Englewood Cliffs, NJ, USA.

65. STATGRAPHICS Centurion XV, sofware, (2005). StatPoint, Inc., Statgraphics Centurion XV, Herndon, VA, USA. 2005.

66. Busetti F, Heitz A, Cuomo M, Badoer S, Traverso P (2006) Determination of sixteen polycyclic aromatic hydrocarbons in aqueous and solid samples from an Italian wastewater treatment plant. Journal of Chromatography A 1102: 104-115.

67. Papadaki M, Emery RJ, Abu-Hassan MA, Diaz-Bustos A, Metcalfe IS (2004) Sonocatalytic oxidation processes for the removal of contaminants containing aromatic rings from aqueous effluents. Separation and Purification Technology 34: 35-42.

68. Psillakis E, Ntelekos A, Mantzavinos D, Nikolopoulos E, Kalogerakis N (2003) Solid-phase microextraction to monitor the sonochemical degradation of polycyclic aromatic hydrocarbons in water. Journal of Environmental Monitoring 5: 135-140.

69. Psillakis E, Goula G, Kalogerakis N, Mantzavinos D (2004) Degradation of polcyclic aromatic hydrocarbons in aqueous solutions by ultrasonic irradiation. Journal of Hazardous Materials B 108: 95-102.

70. Chakinala AG, Gogate PR, Burgess AE, Bremner DH (2008a) Treatment of industrial wastewater effluent using hydrodynamic cavitaation and the advanced fenton process. Ultrasonics Sonochemistry 15: 49-54.

71. Chakinala AG, Gogate PR, Chand R, Bremner DH, Molina R (2008b) Intensification of oxidation capacity using chloroalkanes as additives in hydrodynamic and acoustic cavitation reactors. Ultrasonics Sonochemistry 15: 164-170.

72. Rokhina EV, Lens P, Virkutyte J (2009) Low-frequency ultrasound in biotechnology: State of the art Trends Biotechnology 27: 298-306.

73. David B (2009) Sonochemical degradation of PAH in aqueous solution. Part I: Monocomponent PAH solution. Ultrasonics Sonochemistry 16: 260-265.

74. Kidak R, Wilhelm A-M, Delmas H (2009) Effect of process parameters on the Energy requirement in ultrasonical treatment of waste sludge. Chemical Engineering and Processing: Process Intensification 48: 1346-1352.

75. De Visscher A, Van Eeenoo P, Drijvers D, Van Langenhove H (1996) Kinetic model for the sonochemical degradation of monocyclic aromatic compounds in aqueous solution. The Journal of Physical Chemistry 100: 11636-11642.

76. Dewulf J, Van Langenhove H, De Visscher A, Sabbe S (2001) Ultrasonic degradation of trichloroethylene and chlorobenzene at micromolar concentrations: Kinetics and modelling. Ultrasonics Sonochemistry 8: 143-150.

77. Minnaert M (1933) On musical air bubbles and the sounds of running water. Philosophical Magazine 16: 235-248.

78. Burdin F, Tsochatzidis NA, Guiraud P, Wilhelm A-M, Delmas H (1999) Characterisation of the acoustic cavitation cloud by two laser techniques. Ultrasonics Sonochemistry 6: 43-51.

79. Cum G, Galli G, Gallo R, Spadaro A (1992) Role of frequency in the ultrasonic activation of chemical reactions. Ultrasonics 30: 267-270.

80. Wang J, Ma T, Zhang Z, Zhang X, Jiang Y (2006a) Investigation on the sonocatalytic degradation of parathion in the presence of nanometer rutile titanium dioxide (TiO2) catalysis. Journal of Hazardous Materials B 137: 972-980.

81. Wang J, Pan Z, Zhang Z, Zhang X, Wen F (2006b) Sonocatalytic degradation of methyl parathion in the presence of nanometer and ordinary anatase titanium dioxide catalysts and comparison of their sonocatalytic abilities. Ultrasonics Sonochemisty 13: 493-500.

82. Sivakumar M, Pandit AB (2001) Ultrasound enhanced degradation of Rhodamine B: Optimization with power density. Ultrasonics Sonochemistry 8: 233-240.

83. Suslick KS (1986) Organometallic sonochemistry, in advances in organometallic chemistry, New York: Academic Pres 73-119.

84. Entezari MH, Sharif Al-Hoseini Z (2007) Sono-sorption as a new method for the removal of Methylene Blue from aqueous solution. Ultrasonics Sonochemistry 14: 599-604.

85. Oztekin R, Sponza DT (2009a) Effect of sonication on the treatment of polycyclic aromatic hydrocarbons (PAHs) in a petrochemical industry wastewater and toxicity evaluations 26: 14-20.

86. Oztekin R, Sponza DT (2009b) Effect of sonication on the treatment of PAHs and toxicity in a petrochemical industry wastewater 33: 213-217.

87. Oztekin R, Sponza DT (2012) Treatment of wastewaters from the olive mill industry by sonication. Journal of Chemical Technology and Biotechnology 88: 212-225.

88. Sponza DT, Oztekin R (2009a) Effect of ultrasonic irradiation on the treatment of poly-aromatic substances (PAHs) from a petrochemical industry wastewater 33: 109-116.

89. Sponza DT, Oztekin R (2009b) Effect of ultrasound on the treatment of petrochemical industry wastewaters, Proceedings of National Environmental Engineering Congress, 8. Environment Engineering Chamber, Antalya, Turkey, 12th-14th November 2009: 217-236.

90. Sponza DT, Oztekin R (2010a) Effect of sonication assisted by titanium dioxide and ferrous ions on polyaromatic hydrocarbons (PAHs) and toxicity removals from a petrochemical industry wastewater in Turkey. Journal of Chemical Technology and Biotechnology 85: 913-925.

91. Sponza DT, Oztekin R (2010b) Removals of PAHs and acute toxicity via sonication in a petrochemical industry wastewater. Chemical Engineering Journal 162: 142-150.

92. Sponza DT, Oztekin R (2010c) Destruction of some more and less hydrophobic PAHs and their toxicities in a petrochemical industry wastewater with sonication in Turkey, Bioresource Technology 101: 8639-8648.

93. Sponza DT, Oztekin R (2011) Removals of some hydrophobic poly aromatic hydrocarbons (PAHs) and Daphnia magna acute toxicity in a petrochemical industry wastewater with ultrasound in Izmir-Turkey. Separation and Purification Technology 77: 301-311.

94. He Z, Lin L, Song S, Xia M, Xu L (2008) Mineralization of C.I. Reactive Blue 19 by ozonation combined with sonolysis: Performance optimization and degradation mechanism. Separation and Purification Technology 62: 376-381.

95. Ince NH, Tezcanli-Guyer G (2004) Impacts of pH and molecular structure on ultrasonic degradation of azo dyes. Ultrasonics 42: 591-596.

96. Tauber A, Mark G, Schuchmann H-P, von Sonntag C (1999a) Sonolysis of tert-butyl alcohol in aqueous systems. Ultrasonics Sonochemistry 9: 291-296.

97. Tauber A, Mark G, Schuchmann H-P, von Sonntag C (1999b) Sonolysis of tert-butyl alcohol in aqueous solution. Journal of Chemical Society Perkin Transactions 2: 1129-1135.

98. Zhao S, Li J, Wang L, Wang X (2010) Degradation of Rhodamine B and Safranin-T by MoO3:CeO2 Nanofibers and Air Using a Continuous Mode. Clean-Soil, Air, Water 38: 268-274.

99. Vankar PS, Shanker R (2008) Ecofriendly ultrasonic natural dyeing of cotton fabric with enzyme pretreatments. Desalination 230: 62-69.

100. Vassilakis C, Pantidou A, Psillakis E, Kalogerakis N, Mantzavinos D (2004) Sonolysis of natural phenolic compounds in aqueous solutions: degradation pathways and biodegradability. Water Research 38: 3110-3118.

101. Currell DL, Wilhelm G, Nagy S (1963) The effect of certain variables on the ultrasonic cleavage of phenol and of pyridine. Journal of the American Chemical Society 85: 127-130.

102. Atanassova D, Kefalas P, Petrakis C, Mantzavinos D, Kalogerakis N (2005) Sonochemical reduction of the antioxidant activity of olive mill wastewater. Environment International 31: 281-287.

103. Moore SB, Ausley LW (2004) Systems thinking and green chemistry in the textile industry: Concepts, technologies and benefits. Journal of Cleaner Production 12: 585-601.

104. Ghodbane H, Hamdaoui O (2009) Intensification of sonochemical decolorization of anthraquinonic dye Acid Blue 25 using carbon tetrachloride. Ultrasonics Sonochemistry 16: 455-461.

105. Behnajady MA, Modirshahla N, Bavili Tabrizi S, Molanee S (2008a) Ultrasonic degradation of Rhodamine B in aqueous solution: Influence of operational parameters. Journal of Hazardous Materials 152: 381-386.

106. Behnajady MA, Modirshahla N, Shokri M, Vahid B (2008b) Effect of operational parameters on degradation of Malachite Green by ultrasonics irradiation. Ultrasonics Sonochemistry 15: 1009-1014.

107. Sayan E (2006) Optimization and modeling of decolorization and COD reduction of reactive dye solutions by ultrasound-assisted adsorption. Chemical Engineering Journal 119: 175-181.

108. Petrier C, Francony A (1997) Ultrasonic wastewater treatment: Incidence of ultrasonic frequency on the rate of phenol and CCl4 degradation. Ultrasonics Sonochemistry 4: 295-300.

109. Takizawa Y, Akama M, Yoshihara N, Nojima O, Arai K (1996) Hydroxylation of phenolic compounds under the condition of ultrasound in aqueous solution. Ultrasonics Sonochemistry 3: 201-204.

110. Ince NH, Tezcanli G, Belen R, Apikyan IG (2000) Ultrasound as a catalyzer of aqueous reaction systems: the state of the art and environmental applications, Applied Catalyst B: Environment 29: 167-176.

111. Masui, T, Ozaki T, Machida K, Adachi G (2000) Preparation of Ceria-Zirconia sub-catalysts for automotive exhaust cleaning. Journal of Alloys and Compounds 303-304: 49-55.

112. Hendriksen BLM, Ackermann MD, Van Rijn R, Stoltz D, Popa I (2010) The Role of Steps in Surface Catalysis and Reaction Oscillations. Nature Chemistry 2: 730-734.

113. Arun Kumar D, Selvasekarapandian S, Nithya H, Masuda Y (2012) Structural and conductivity analysis on cerium fluoride nanoparticles prepared by sonication assisted method. Solid State Sciences 14: 626-634.

114. Li Y, Chen J, Liu J, Ma M, Chen W (2010) Activated carbon supported TiO_2-photocatalysis doped with Fe ions for continuous treatment of dye wastewater in a dynamic reactor. Journal of Environmental Sciences 22: 1290-1296.

115. Zhao B, Shi B, Zhang X, Cao X, Zhang Y (2011) Catalytic wet hydrogen peroxide oxidation of H-acid in aqueous solution with TiO_2-CeO_2 and Fe/TiO_2-CeO_2 catalysts. Desalination 268: 55-59.

116. You J, Chen F, Zhao X, Chen Z (2010) Preparation, characterization and catalytic oxidation property of CeO_2/Cu^{2+}- attapulgite (ATP) nanocomposites. Journal of Rare Earths 28: 347-352.

117. Li C, Chen R, Zhang X, Shu S, Xiong J (2011) Electrospinning of CeO_2-ZnO composite nanofibers and their photocatalytic property. Materials Letters 65: 1327-1330.

118. Anwer H, Mahmood A, Lee J, Kim K-H, Park J-W (2019) Photocatalysts for degradation of dyes in industrial e_uents: Opportunities and challenges. Nano Res 12: 955-972.

119. Zangeneh H, Zinatizadeh AAL, Habibi M, Akia M, Isa MH (2015) Photocatalytic oxidation of organic dyes and pollutants in wastewater using di_erent modified titanium dioxides: A comparative study. J Ind Eng Chem 26: 1-36.

120. Fornasiero P, Balducci G, Monte RD, Kaspar J, Sergo V (1996) Modification of the redox behaviour of CeO_2 induced by structural doping with ZrO_2. J.Catal 164: 173-183.

121. Sahibzada M, Steele BCH, Zheng K, Rudkin RA, Metcalfe IS (1997) Development of solid oxide fuel cells based on a Ce(Gd)O_2−x electrolyte film for intermediate temperature operation. Catalysis Today 38: 459-466.

122. Bernal S, Calvino JJ, Cauqui MA, Gatica JM, CLarese C (1999) Some recent results on metal/support interaction effects in NM/CeO_2 (NM: noble metal) catalysts. Catalysis Today 50: 175-206.

123. Rossignol S, Madier Y, Duprez D (1999) Preparation of zirconia±ceria materials by soft chemistry. Catalysis Today 50: 261-270.

124. Trovarelli A, Leitenburg CD, Dolcetti G (1997) Design better cerium-based oxidation catalysts. Chem Tech. 27: 32-40.

125. Morozova LV, Lapshin AE, Glushkova VB (2002) Preparation and Properties of a Ceramic in the ZrO_2 -CeO_2 System. Refractories and Industrial Ceramics 43:179-180.

126. Shiono M, Kobayashi K, Nguyen TL, Hosoda K, Kato T (2004) Effect of CeO_2 interlayer on ZrO_2 electrolyte / La(Sr)CoO_3 cathode for low-temperature SOFCs. Solid State Ionics 170: 1-7.

127. Yahiro H, Bab Y, Eguchi K, Arai H (1988) High Temperature Fuel Cell with Ceria-Yttria Solid Electrolyte. Journal of The Electrochemical Society 135: 2077-2079.

128. Orel Z, Orel B (1994) Optical Properties of Pure CeO2 and Mixed CeO2/SnO2 Thin Film Coatings. Phys. Status Solidi B 186: 33-36.

129. Esch F, Fabris S, Zhou L, Montini T, Africh C (2005) Electron localization determines defect formation on ceria substrates. Science 309: 752-755.

130. Yue L, Zhang X-M (2009) Structural characterization and photocatalytic behaviours of doped CeO_2 nanoparticles. J Alloys Compd 475: 702-705.

131. Wang J, Jiang Y, Zhang Z, Zhang X, Ma T (2007) Investigation on the sonocatalytic degradation of Acid Red B in the presence of nanometer TiO_2 catalysts and comparison of catalytic activities of anatase and rutile TiO_2 powders. Ultrasonics Sonochemistry 14: 545-551.

132. Laxmi PNV, Sarithaa P, Rambabua N, Himabindua V, Anjaneyulu Y (2010) Sonochemical degradation of 2-chloro-5methyl phenol assisted by TiO_2 and H_2O_2. Journal of Hazardous Materials 174: 151-155.

133. Han WY, Zhu WP, Zhang PY, Li LS (2004) Photocatalytic degradation of phenols in aqueous solution under irradiation of 254 and 185 nm UV light. Catalysis Today 90: 319-324.

134. Robbins MD, Henderson MA (2006) The partial oxidation of isobutene and propene on TiO_2(110). Journal of Catalysis 238: 111-121.

135. Yang S, Zhu W, Wang J, Chen Z (2008) Catalytic wet air oxidation of phenol over CeO_2-TiO_2 catalyst in the batch reactor and the packed-bed reactor. Journal of Hazardous Materials 153: 1248-1253.

136. Gao X, Jiang Y, Fu Y, Zhong Y, Luo Z (2010) Preparation and characterization of CeO_2/TiO_2 catalysts for selective catalytic reduction of NO with NH_3. Catalysis Communications 11: 465-469.

137. Deng S, Li Z, Huang J, Yu G (2010) Preparation, characterization and application of a Ce-Ti oxide adsorbent for enhanced removal of arsenate from water. Journal of Hazardous Materials 179: 1014-1021.

138. Yang SX, Zhu WP, Jiang ZP, Chen ZX, Wang JB (2006) The surface properties and the activities in catalytic wet air oxidation over CeO_2-TiO_2 catalysts. Applied Surface Science 252: 8499-8505.

139. Shirsath SR, Pinjari DV, Gogate PR, Sonawane SH, Pandit AB (2013) Ultrasound assisted synthesis of doped TiO_2 nano-particles: Characterization and comparison of effectiveness for photocatalytic oxidation of dyestuff effluent. Ultrasonics Sonochemistry 20: 277-286.

140. Wang J, Lv Y, Zhang L, Liu B, Jiang R, et al. (2010) Sonocatalytic degradation of organic dyes and comparison of catalytic activities of CeO_2/TiO_2, SnO_2/TiO_2 and ZrO_2/TiO_2 composites under ultrasonic irradiation. Ultrasonics Sonochemistry 17: 642-648.

141. Liu H, Wang M, Wang Y, Liang Y, Cao W (2011) Ionic liquid-templated synthesis of mesoporous CeO_2-TiO_2 nanoparticles and their enhanced photocatalytic activities under UV or visible light. Journal of Photochemistry and Photobiology A: Chemistry 223: 157-164.

142. Wang J, Zhou G, He R, Huang W, Zhu J (2020) Experimental preparation and optical properties of CeO_2/TiO_2 heterostructure, Journal of Materials Research and Technology 9: 9920-9928.

Henry Journal of Acupuncture & Traditional Medicine

Henry Journal of Anesthesia & Perioperative Management

Henry Journal of Aquaculture and Technical Development

Henry Journal of Cardiology & Cardiovascular Medicine

Henry Journal of Case Reports & Imaging

Henry Journal of Cell & Molecular Biology

Henry Journal of Tissue Biology & Cytology

Henry Journal of Clinical, Experimental and Cosmetic Dermatology

Henry Journal of Diabetes & Metabolic Syndrome

Henry Journal of Emergency Medicine, Trauma & Surgical Care

Henry Journal of Haematology & Hemotherapy

Henry Journal of Immunology & Immunotherapy

Henry Journal of Nanoscience, Nanomedicine & Nanobiology

Henry Journal of Nutrition & Food Science

Henry Journal of Obesity & Body Weight

Henry Journal of Cellular & Molecular Oncology

Henry Journal of Ophthalmology & Optometry

Henry Journal of Perinatology & Pediatrics

Submit Your Manuscript: https://www.henrypublishinggroups.com/submit-manuscript/

Henry Publishing Groups, 41341 Red Birch Dr, Aldie, VA, 20105, USA

Tel: +1 571-275-4480; E-mail: contact@henrypublishinggroups.org

https://www.henrypublishinggroups.com/